Progress and Perspectives on Phononic Crystals

Thomas Vasileiadis,[1] Jeena Varghese,[1] Visnja Babacic,[1] Jordi Gomis-Bresco,[2] Daniel Navarro Urrios,[2] and Bartlomiej Graczykowski[1]

[1)] *Faculty of Physics, Adam Mickiewicz University, Uniwersytetu Poznanskiego 2, 61-614 Poznan, Poland*

[2)] *Departament de Física Aplicada, Universitat de Barcelona, IN2UB, Barcelona 08028, Spain.*

(Dated: 30 December 2020)

Phononic crystals (PnCs) control the transport of sound and heat similarly to the control of electric currents by semiconductors and metals or light by photonic crystals. Basic and applied research on PnCs spans the entire phononic spectrum, from seismic waves and audible sound to gigahertz phononics for telecommunications and thermal transport in the terahertz range. Here, we review the progress and applications of PnCs across their spectrum, and we offer some perspectives in view of the growing demand for vibrational isolation, fast signal processing, and miniaturization of devices. Current research on macroscopic low-frequency PnCs offers complete solutions from design and optimization to construction and characterization of, e.g., sound insulators, seismic shields and ultrasonic imaging devices. Hypersonic PnCs made of novel low-dimensional nanomaterials can be used to develop smaller microelectromechanical systems and faster wireless networks.

I. INTRODUCTION

In 1932, Frenkel[1] used the term phonon to describe a quantum of the acoustic field, a new hypothetical particle introduced two years earlier by Tamm.[2] The word phonon originates in Greek φωνή (phonē, meaning voice) and it is an analogy to a photon being the quantum of the electromagnetic field. Needless to say that the importance of phonons in fundamental and applied research goes far beyond the common understanding of sound. The full phononic spectrum spans a broad, mostly inaudible, range of frequencies from a few millihertz up to dozens of terahertz. In general, the phononic spectrum (Fig. 1) consists of infrasounds (<few Hz), audible sound (from few Hz to 20 kHz), ultrasounds (from 20 kHz to 1 GHz), hypersounds (from 1 GHz to 1 THz) and heat ($\gtrapprox$ 1 THz at room temperature). For all these bands, acoustic waves/phonons are information and energy carriers that play an inherent role in condensed matter physics. The properties of the hosting medium dictate two fundamental features of phonons, i.e., their dispersion relation (spectral and spatial) and mean free path (lifetime, attenuation).[3,4] For bulk, homogeneous solids, one can distinguish three orthogonal modes (polarizations) of acoustic phonons: one (fast) longitudinal and two (slow) transverse phonons. At wavelengths much longer than the interatomic distances, all three modes are non-dispersive (phase and group velocities are independent of the momentum), typically up to hundreds of GHz. Hence, classical elastodynamics is sufficient to determine the phonon velocities.[5]

To alter the phonon propagation, one can employ spatial confinement and modulation of the material. The former approach turns bulk acoustic waves (BAWs) into surface acoustic waves (SAWs) propagating in close vicinity of free surfaces (Rayleigh, Sezawa, and Love waves) or Lamb waves in free-standing slabs and membranes.[6] The second strategy was successfully realized in Phononic Crystals (PnCs), i.e., synthetic materials with periodic modulation of elastic properties utilizing the wave-like nature of phonons. The structure of PnCs mimics the arrangement of atoms in natural crystals and results in phononic features typical for thereof. These are: the appearance of the second-order Brillouin zones, modification of the phonon dispersion, zone folding, and band gaps due to Bragg reflections. In addition to Bragg gaps (BG), the so-called hybridization gaps (HG) can appear when the periodic scatterers are made of mechanical resonators such as pillars, spheres, or stripes. The avoided crossing of the localized modes and propagating waves leads to sub- or super-wavelength stop bands robust to the PnC lattice imperfections.[7–12]

The first theoretical proposals for 2D acoustic band gap materials were published almost simultaneously by Sigalas and Economu,[13] and Kushwaha et al.[14] Notably, one has to give credit to much earlier works from the 70s and 80s on the propagation of SAWs in periodically corrugated surfaces, being in fact 1D PnCs.[15–17] The last three decades have faced a flourishing of theoretical and experimental research on PnCs in the full phononic spectrum. Quite often, these studies were inspired by the achievements of the more mature fields of photonics and electronics. Nevertheless, the field of PnCs has introduced its original concepts employing the nature of phonons, their coupling with other elementary excitations, and their inseparable connection with the condensed matter.[7–12,18]

This paper presents an experimentalists' point of view on the recent progress and prospects of PnCs. We present an overview of the advances in fabrication, experimental characterization, and new features for the broad spectrum of acoustic waves/phonons. The paper is organized as follows: First, we consider macroscopic PnCs aiming at manipulation of sub-GHz waves (infrasound, sound, and ultrasound). Second, we focus on PnCs of a sub-micrometer feature size operating at GHz frequencies (hypersound). Third, we consider THz photon – GHz phonon coupling, both at sub-micrometer wavelengths, in periodic phononic-photonic crystals (phoxonic, optomechanical crystals). Fourth, we discuss the role of THz phonons as the heat carrier in periodically modulated structures. Finally, we cover recent advances and prospects of topological phononics in a broad spectrum of frequencies.

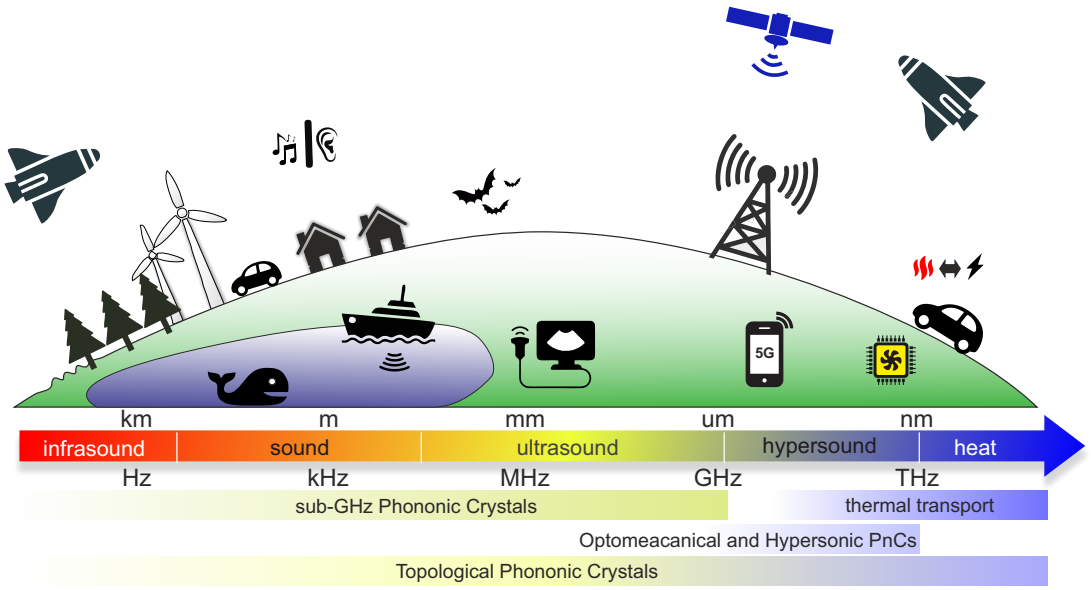

FIG. 1. The phononic spectrum - some natural and human-made sources of acoustic waves/phonons relevant for the considered applications of phononic crystals.

II. SUB-GIGAHERTZ PHONONIC CRYSTALS

Since the earlier works on sonic band gap crystals,[19,20] research on PnCs and acoustic metamaterials (AMMs) in the sub-GHz frequency spectrum is an active domain with promising applications. First, the technological advances in additive manufacturing (3D printing) offered a great solution to transfer many intricate theoretical designs into laboratory-scale structures. The challenges of practical applications can be resolved with auxetic metamaterials, acoustic metasurfaces, tunable and multifunctional AMMs. In particular, widening the locally resonant band gaps of periodic structures can improve the performance of seismic shields, ultrasonic waveguides and other phononic devices. Sub-GHz phononics need a heterogeneous community to bring together the concepts of several scientific disciplines: device physics, geology, mathematics, civil engineering, electronics and telecommunications, to name a few. Here, we address the possible directions of phononic materials research for manipulating seismic waves, sound, and ultrasonic waves with the feature size ranging from a few meters to micrometer scale, respectively. Theoretical PnC designs are out of the scope of this perspective, and a detailed review on PnCs and AMMs can be found in other articles.[4,21–26]

The practical size limitation of PnCs is enough to motivate locally resonant structures for ultra-low frequency applications. However, functional sub-wavelength scale PnCs need improvement regarding compactness, weight and cost effectiveness. For example, a metabarrier consisting of few-meter-sized resonant structures (cylindrical mass in concrete slabs)[27] can convert the seismic Rayleigh surface waves (RSWs) to shear BAWs that attenuate on the soil surface. Such locally resonant structures are widely used as seismic shields/insulators[27–29] in the configurations like inclusions in the soil[28,30] or buried mass resonators.[31,32] Interestingly, AMMs are not strictly artificial. A forest of trees can act as natural PnC[33–35] [Fig. 2 (a)] and offers large attenuation of seismic RSWs and shear waves (S-waves) in the broad frequency range below 150 Hz [Fig. 2 (b)]. Graded vertical pillars arranged on an elastic substrate can block RSWs by reflecting them (classical wedge showing rainbow effect) or by converting them to BAWs (inverse wedge).[36] These experiments have to be realized in the geological scale and they involve designing tree wedges with height varying profiles and artificial vertical pillars for seismic protection. However, the potential of each design depends on the geometry of the structure and the viscoelastic properties of the soil.[31]

While numerous theoretical models[21,31,46–48] of phononic structures in various geometries and dimensions are available, the experimental realization is still challenging. Fabrication methods experience several limitations in terms of low-cost raw material choice, minimum feature size, aspect ratios, or support requirements.[49] Additive manufacturing technologies, including stereolithography, material jet printing, fused deposition modeling, microlaser sintering/melting make the design of 3D sonic PnCs much more feasible in the millimeter scale.[49–52] Rainbow metamaterials are one of the best examples of structures with broad and robust sonic band gaps.[53] Such systems with lightweight structures were first observed in the context of optical waves,[54] and were further expanded to realize their acoustic analogs. Chen et al.[55] have designed a gradient metamaterial beam for the enhancement of flexural waves. Disorder induced bandgap tuning has been studied using a 3D printed cantilever-in-mass design showing the wave trapping effect.[51] This study revealed that mistuning in the design of the metamaterial can destroy its band gaps. In some

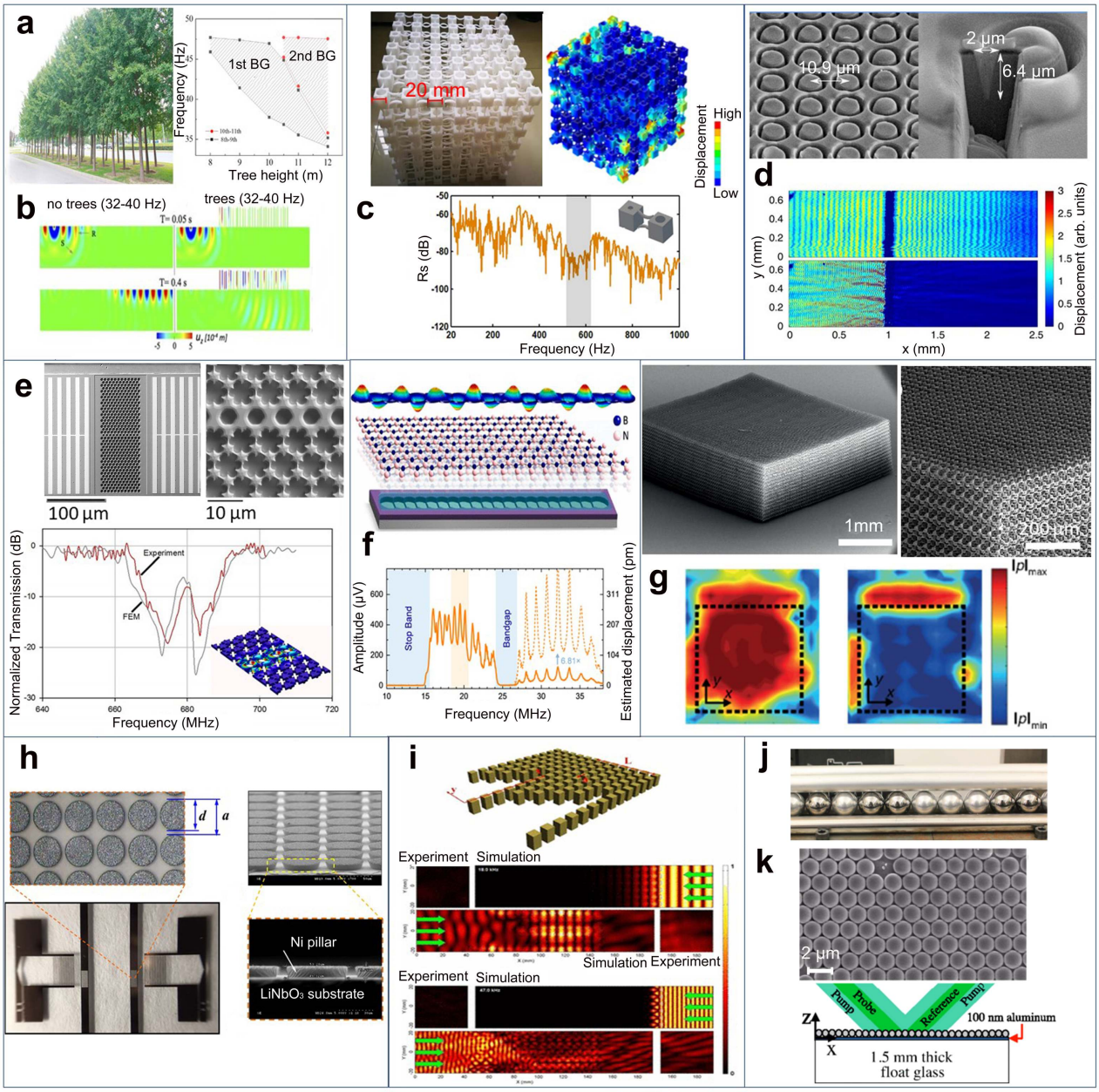

FIG. 2. Sub-GHz phononic materials: (a) natural PnC made of trees[35] and (b) filtering of seismic Rayleigh and S-waves.[33] (c) 3D sonic rainbow metamaterial[37] and (d) annular hole PnC.[38] Waveguides made of (e) SiC – air PnC in a hexagonal lattice,[39] (f) h-BN coupled resonator arrays,[40] (g) microlattice for ultrasonic transmission.[41] Pillar PnC arrays for (h) acoustofluidics[42] and (i) acoustic diode.[43] Tunable granular crystals: (j) macroscopic bead array of steel-aluminum spheres of millimeter size,[44] (k) self-assembled 2D layer of polystyrene particles of 1 μm diameter and the schematic of the pump-probe experimental setup to probe the interactions between spherical particles contact resonances and propagating SAWs.[45] The (a-k) are reproduced with permissions from[33,35,37–45] with copyrights obtained from 2019 Elsevier Ltd./iswcr, 2016 Springer Nature, 2020 Springer Nature, 2017 Springer Nature, 2018 AIP Publishing, 2019 American Chemical Society, 2016 American Physical Society, 2019 Elsevier Ltd., 2011 American Physical Society, 2019 IOP Publishing, 2017 American Physical Society, respectively.

cases, irregularities in the design of PnCs can lead to wider band gaps. For sonic rainbow PnCs [Fig. 2 (c)], a nearly periodic system of cuboids connected by curved beams, shows an attenuation bandwidth twice that of the periodic design of equal mass.[56] Although 3D printing methods have revolutionized microscale structures with complex geometries, a large scale production strategy at low cost is still under development. 4D printing methods is the next game-changer, which may accelerate the scaling-up procedure from laboratory prototypes to large-scale devices.[57] In addition, artificial intelligence (AI) based techniques, like topological optimization and machine learning, may lead to improved design

methodologies.[58–60]

Recently, soft AMMs were introduced to manipulate ultrasonic waves for applications like sub-wavelength imaging, acoustic lenses, and transformation acoustics.[61,62] The design is based on sub-wavelength resonators suspended in an acoustic fluid. Such "soft-gel nature" offers a feasible step towards tunable and responsive AMMs that allows molding the metamaterial in the desired shape, size, and dimensions. 3D ultrasonic metafluid with macroporous microbeads fabricated by soft matter techniques exhibited double negative acoustic impedances. The silicon rubber beads of mean radius 160 μm suspended in the water-based gel matrix act as Mie resonators showing strong monopolar and dipolar resonances. This approach can be exploited on a large scale to produce zero or negative index materials for acoustic imaging applications.[22,24,63,64]

Hierarchial architectures have been used to improve structural integrity and to minimize the amount of material. Several works have explored how the unit cell geometries, lattice material, and dimensions, can tailor the phononic properties.[65–67] A 3D microlattice [Fig. 2 (g)] made by 2-photon lithography can exploit the ultrasonic wave propagation in water by elastoacoustic hybridization. The lattice design with truss-like elements (lattice constant about 70 μm) allows tailoring the HG that effectively attenuates the acoustic waves due to fluid interaction. A very high transmission ($> 80\%$) in the high frequency ultrasonic range (nearly 30 MHz) is observed outside this band gap due to the impedance matching with that of water. This can be further used in biomedical imaging, where smaller penetration depth and higher resolution are important.[41] These microlattices are scalable and can find use as resonators, acoustic insulators, and ultrasonic transducers.[68]

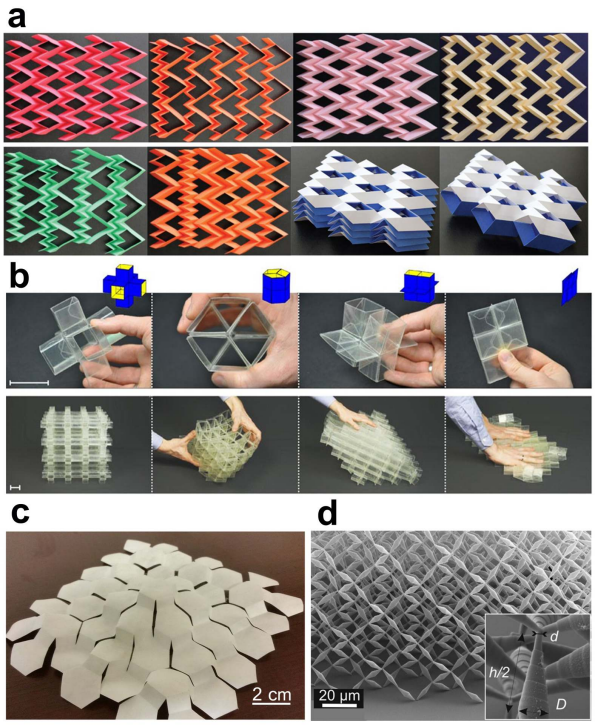

FIG. 3. Reconfigurable metamaterials: Origami inspired metamaterial designs. (a) Unit cells with holes arranged in layers[69], (b) mechanical MMs with cubic microstrctures[70], (c) combining cut fold structures in 2D sheets[71] and (d) pentamode metamaterial[72] design by 3D DLW optical lithography. Figures (a-d) reproduced with permissions from[69–72] and copyrights requested from 2015 AAAS Publishing, 2016 Springer Nature, 2015 PNAS, 2012 AIP Publishing, respectively.

Micro-electro-mechanical systems (MEMS) harnessing RF SAWs are important for signal processing and telecommunications.[73] A standard design of SAW devices is a periodic array of etched holes.[74] However, the band gaps of such systems lie in the frequency range of leaky SAWs. In that sense, locally resonant (LR) structures in composite pillar arrays were used to open low-frequency LR band gaps for SAW propagation.[75] A finite depth annular hole PnC[38] [Fig. 2 (c)] analogous to the pillared architecture revealed potentially improved LR band gaps. The uniform array of holes were fabricated in a lithium niobate ($LiNbO_3$) delay line using focused ion beam (FIB) etching. Moreover, the SAW attenuation has additional geometric freedom compared to the cylindrical pillar designs allowing tailorable SAW dispersions. This design can be exploited where strong acoustic confinement and miniaturization are indispensable. For example, a pillar PnC device [Fig. 2 (h)] made of nickel pillars electroplated on $LiNbO_3$ substrate achieved perfect scattering of standing SAWs (nearly 30 MHz). This generated strong acoustic radiation force and was exploited for concentrating and separating polystyrene microparticles.[42] The annular hole PnC design can be exploited in SAW devices for microfluidics[76–78] and further extended to different particle-size combinations and biomolecules.

The introduction of defect modes in a periodic crystal can trap the acoustic energy. For example, inserting space gaps in a square array of cylindrical pillars improves the performance of demultiplexing and wave filtering.[79] A 2D SiC-air PnC with circular inclusions produced waveguiding at 680 MHz allowing 39% transmission of the acoustic energy [Fig. 2 (e)].[39] Comparison of 90° bend and straight waveguides showed that curved paths produce additional losses.[80] A coupled-resonator array [Fig. 2 (f)] using hexagonal boron nitride PnC (fabricated by the integrative approach of dry exfoliation after FIB etching and patterning) supported the MHz wave propagation over an effective distance of 1.2 mm.[40] The piezoelectric properties of this crystal, and van der Waals layered materials, can be explored further to generate tunable devices for RF applications. Recently a virtual soft boundary based AMM design with resonant tube arrays allowed frequency separation keeping the flow of the medium unaffected.[81] This method can be further explored to design complex functional waveguides and is also viable for microfluidic applications in the future. Waveguides suffer signal losses; future phononic devices have a significant role in achieving better confinement.

Granular crystals, ordered macroscopic beads [Fig. 2 (j)] interacting via adhesion forces exhibited interesting wave propagation characteristics.[82,83] From the experimental veri-

fication of "sonic vacuum"[45,84] these crystals demonstrated non-linear waves (solitons) with strong localization, discrete breathers,[85] rotational elastic wave propagation,[86] and several engineering applications as tunable wave filters, acoustic lenses, switches, and rectifiers.[87,88] The flexibility in terms of size, shape, stiffness, and spatial orientation of solid particles in the lattice makes them easily tailorable for acoustic phenomena. In addition, tunability in terms of precompression transformed the wave propagation from a highly non-linear regime (with no compression) to a nearly linear regime (with precompression).

Self-assembling has enabled scaling down granular crystals to micron feature size large area/volume structures. In such systems (example in [Fig. 2 (k)]), laser pump-probe experiments (transient grating technique) revealed a critical role of interparticle and particle-substrate bonding due to adhesion in forming acoustic band gaps for SAWs and Lamb waves.[89,90] Notably, even disordered 2D granular crystals could effectively attenuate SAWs near their resonant frequency, serving as a perfect metamaterial for wave attenuation and filtering.[91] Compared with commonly used pillar resonant structures, microgranular crystals are weakly adhered to the substrate. In perspective, the resonant frequency can be tailored by the inter-particle and particle-substrate contacts via temperature or hydrostatic pressure treatments below the glass transition temperature.[92,93] A complex contact dynamics of SAW attenuation was explained by Hiraiwa for tailored microspheres using scanned laser ultrasonics.[94] The interparticle stiffness was modified via the deposition of a thin aluminum film over the monolayer, ultimately exhibiting horizontal-rotational contact resonances in addition to vertical resonances. This improved the attenuation regime opening additional band gap at the lower resonances. Recently, splitting of the spheroidal contact resonance resulting from the symmetry breaking of the substrate was explained.[45] These studies can lead to engineering of SAWs devices such as filters, sensors and waveguides. In addition, advances in self-assembly enable scaling down to nanosphere dimensions, opening a broad horizon to manipulate wave propagation in the hypersonic regime (see section 3).

An important aspect of phononic materials, which broadens their potential applications, is tunability. Some examples are self-modulated metamaterials,[95–97] Helmholtz resonators,[98] membranes,[99,100] fluid-filled hollow pillars (whispering gallery modes),[101] split ring resonators,[102] piezoelectric materials,[103,104] decorated membrane resonators (DMRs),[105] and electromagnetic field controls.[106,107] Some studies have also focused on flexible origami and kirigami-inspired – cut and folded metamaterials[70] [Fig. 3 (a-c)]. A waveguide[108] designed for audible frequency proposed a broad working band and switchable sound propagation. Pentamode metamaterials [Fig. 3 (d)] having their rigidity maintained about the point contacts of elongated unit cells show that their bulk and shear nature is essentially decoupled.[72,109] Several of such designs can be proposed by virtue of their richness in deformation modes. We also envision that bio-inspired and natural PnCs and AMMs will become a more intensive field of study.[110–112] Overall, the future of sub-GHz phononics is vested in active and reconfigurable structures.

III. HYPERSONIC PHONONIC CRYSTALS

The frequency of one gigahertz is the conventional boundary between ultrasounds and hypersounds that can also be assumed in the description of PnCs. Due to their small feature size, which is typically less than one micrometer, the fabrication, experimental characterization and applications of hypersonic PnCs differ significantly from those of sub-GHz PnCs. Hypersonic PnCs can be potentially useful for the development of high-frequency signal processing devices for wireless communications. Nowadays, the operational frequency of wireless communications is in the order of 1 GHz. The future front-end modules have to manage signals from a few to hundreds of GHz to reach the requirements of the next-generation wireless networks. For this purpose, hypersonic PnCs can be implemented as BAW, SAW and Lamb waves filters, according to their architecture.

A. Hypersonic phononic crystals in various dimensions

Three-dimensional (3D) hypersonic PnCs allow tailoring of BAWs dispersion employing Bragg reflections and local resonances similarly to sub-GHz PnCs. To date, a vast variety of 3D PnCs were fabricated employing self-assembling of monodispersed sub-micrometer particles into colloidal crystals (CCs). As in the case of sub-GHz PnCs, the key advantages of CCs are their large volume, low-cost and low-effort fabrication, maintaining high-quality translational order. Also, the forbidden range of frequencies can be adjusted by the NPs size and material, and the material of the matrix .

The first experimental observation of GHz band gaps was reported by Cheng et al.[113] in solid/liquid PnCs. The structures were made of polystyrene (PS) nanoparticles (NPs) self-assembled into face-centered-cubic (fcc) CCs and infiltrated with various fluids. Notably, the observed BG (at about 5 GHz) offered some degree of tuneability by the NPs size and the infiltrated fluid type. Figure 4 (a) displays an example of a solid/solid PnC that was fabricated from self-assembled PS NPs embedded in polydimethylsiloxane (PDMS) matrix.[114] The band diagram and transmission spectrum calculated for this material revealed both BG and HG. However, the experimental data confirmed only the former type centered at about 4 GHz. In addition to the geometry and material parameters, the phononic dispersion of CC PnCs can be tailored by bondings between the NPs. This effect and filtering due to the local resonances were reported for CCs made of silica NPs.[115] For this material, the femtosecond pump-probe technique revealed a long-living mode at 7.5 GHz matching the center of the calculated band gap. It was demonstrated that the sintering of silica NPs could modify this stop band.

The reduction of CC's symmetry results in higher acoustic anisotropy of PnCs. This effect was observed for CCs fabricated from non-spherical NPs, i.e., nanoellipsoids depicted in Fig. 4 (b). In such PnCs, the phononic dispersion [Fig. 4

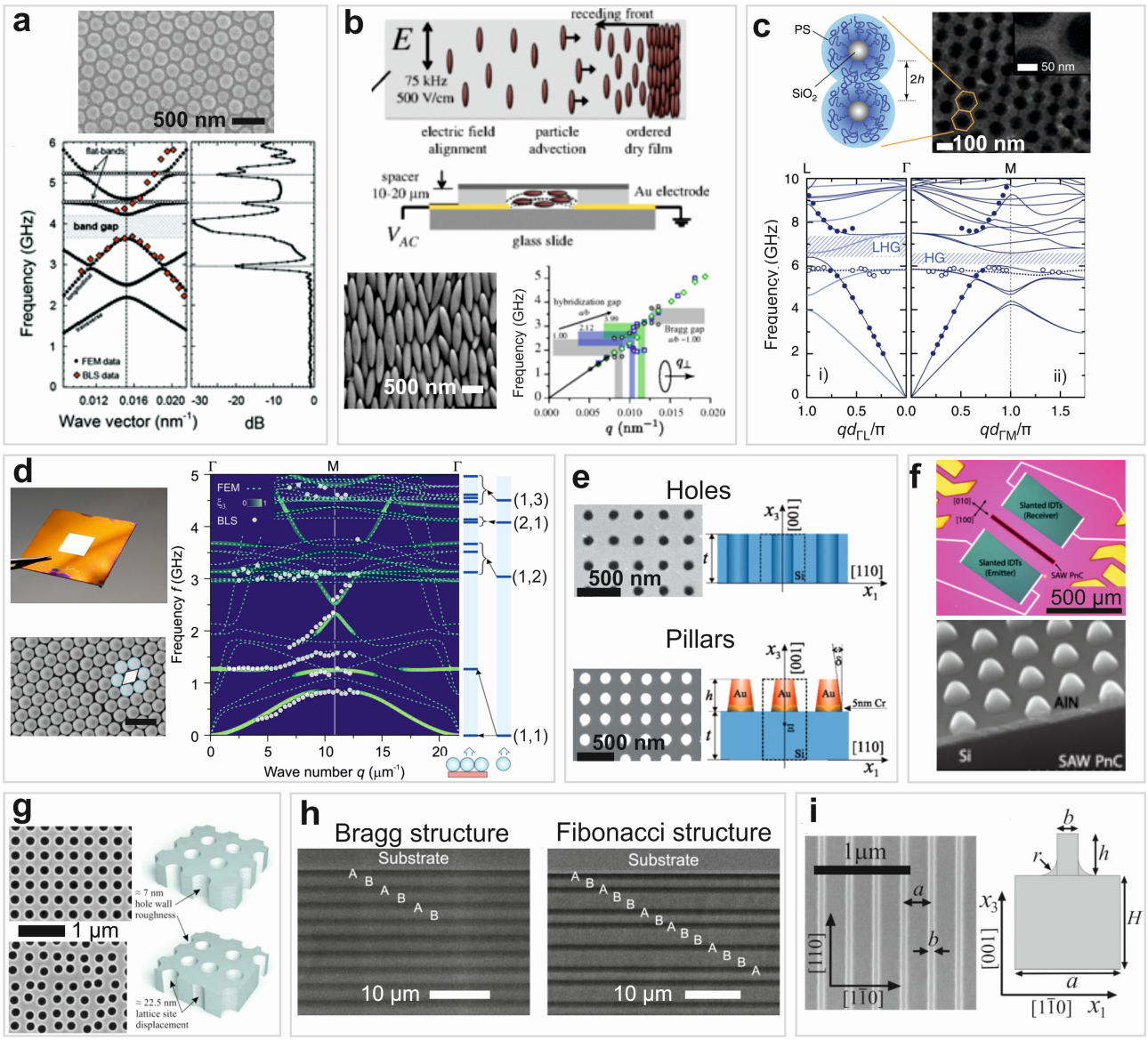

FIG. 4. (a) 3D PnC made of PS spheres embedded in solid PDMS matrix and corresponding band structure.[114] (b) 3D PnC realized of carboxylate modified PS nanoellipsoids. Phononic band diagrams for the $q_{\perp}$ propagation directions when $\alpha/b = 2.12$ (blue squares), $\alpha/b = 3.99$ (green diamonds) and for $\alpha/b = 1$ (black circles).[116] (c) PS brush-grafted silica NPs assembly; Dispersion calculated along (i) [111] shows non-degenerate longitudinal (dark solid lines), double degenerate transverse (light solid lines) and deaf bands (dotted lines); (ii) [112] shows non-degenerate of mixed character and the flat band. Hybridization gaps LHG (for longitudinal modes) and HG (for all modes) are indicated with shaded areas.[117] (d) 2D PnC composed of single layer PS nanoparticles self-assembled on a thin Si_3N_4 membrane, and related dispersion relation.[118] (e) Solid-air and solid-solid 2D PnC fabricated by making a pattern of holes and pillars in/on a thin Si membrane, respectively.[119] (f) Optical image of the device showing a ribbon of the SAW PnC between emitter and receiver (top). SEM image of the cross section of 2D pillar-based SAW-PnC structure (bottom).[120] (g) SEM images of 2D PnC with ordered (top) and disordered pattern of holes (bottom) in Si membrane.[121] (h) Bragg structure made of periodically altering layers of Si with different porosity (left) and quasi periodic Fibonacci structure (right) formed by stacking layers according to Fibonacci sequence.[122] (i) 1D SAW PnC realized by rectangular-like periodic grooves on the (001) surface of crystalline silicon.[123] In (a-d) the experimental dispersion relations (full/open points) were measured by Brillouin light scattering and calculated by finite element method (FEM). Panel (a) shows a calculated transmission spectrum. Figures (a-i) are reproduced with permissions from Refs. 114, 116–123 and copyrights obtained from 2013 American Physical Society, 2014 American Physical Society, 2015 Springer Nature, 2020 American Chemical Society, 2015 American Physical Society, 2018 American Physical Society, 2016 American Chemical Society, 2014 AIP Publishing, and 2014 AIP publishing, respectively.

(b)] can be tuned by changing the NP's aspect ratio, which leads to unidirectional HG.[116] The symmetry reduction of PnCs was also achieved by directional deformation of flexible solid/solid CCs. This was demonstrated for PS–PDMS CCs stretched along the $[1\bar{1}1]$ direction. In this case, the unidirectional expansion of about 17% resulted in the red-shift of the BG. Notably, HGs were found as practically resilient to structural changes.[124] This effect can be utilized in flexible devices that require the performance of PnCs robust to large deformations. In a more general context, HGs are independent of the PnCs' structural imperfections. A recent study has demonstrated a new approach for tunability of HGs in hybrid organic/inorganic PnCs through a complex structure of spherical NPs. The PnCs were composed of self-assembled PS brush-grafted silica NPs with elastic anisotropy across the silica core – polymer shell interface. The spectral position of HGs was adjusted within 5.5-10 GHz range by the degree of polymerization, grafting density, and NP core size [Fig. 4 (c)].[117]

Two-dimensional (2D) hypersonic PnCs have been utilized for altering the propagation of different types of SAWs or Lamb waves. Such systems were designed as 2D periodic patterns on the free surface of bulk or membrane and fabricated employing the bottom-up or top-down approach. The former method is based on large-area 2D CC, i.e., self-assembling of NPs into close-packed monolayers. Figure 4 (d) displays 2D PnCs composed of a PS NPs monolayer deposited on a 50 nm thick Si_3N_4 membrane.[118] For these systems, the measured and calculated phononic dispersion pointed to three distinct types of band gaps for Lamb waves. Namely, they were related to the lattice period (BG), NP-membrane contact resonance (HG), and local resonances of NPs (HG). Notably, the latter type was found to appear in the sub-wavelength (below BG) and super-wavelength (above BG) regimes. The central frequencies of all three types of band gaps can be tuned by particle size, membrane thickness, and adhesion at the NP-NP and NP-membrane interfaces.

The top-down fabrication requires more effort as typically it is based on electron beam lithography (EBL) and reactive ion etching (RIE).[125]. Here, one can distinguish two types of PnCs: solid/air and solid/solid differing in the periodic motifs. The former is realized by the substrate perforation (holes), while the latter by the periodic mass loading (pillars). Both of these schemes were exploited in the PnCs dedicated to SAWs management.[120,126–129] In this case, the frequency stop bands were detuned, in addition to the lattice spacing, by the geometric parameters, i.e., size and shape of holes[130,131] and pillars[119,126,129,132,133] and by solid[134] or liquid inclusions.[130] Figure 4 (e) illustrates two examples of PnCs, i.e., solid/air and solid/solid fabricated from 250 nm thick Si membrane.[119] The solid-air PnC revealed BG for all types of Lamb (waves and BG for symmetric modes, both about 13 GHz. The band diagrams of solid-solid PnC showed apparent hybridization of local resonances of pillars with propagating waves in the membrane, albeit HG was not detected. Overall, 2D PnCs offer a versatile platform for manipulating of confined (SAW, Lamb) acoustic signals in the GHz regime, which can be utilized in wireless communication devices. For example, PnC made from periodically etched silica film on a quartz substrate was demonstrated as a 1.25 GHz one-port Love waves resonator.[128]. In addition, recent work reported piezoelectric and CMOS-compatible pillar-based PnCs [Fig. 4 (f)]. The experimentally measured transmission spectra revealed a 150 MHz wide SAW band gap with the central frequency at about 1.65 GHz.[120]

Both for top-down and bottom-up approaches, the imperfections are an unavoidable issue. Nevertheless, the deviation from the ideal translational order of the lattice can lead to new phononic features. In particular, the disorder can destroy the coherent effects as it was experimentally proved for the example of holey Si membrane illustrated in Fig. 4 (g).[121] Also, theoretical studies revealed that the disorder could result in band gap broadening and acoustic Anderson localization in PnCs.[135,136] Undoubtedly, both works deserve experimental verification in the near future.

One-dimensional (1D) hypersonic PnCs are relatively less complex structures than previously discussed 2D and 3D PnCs. However, they can offer distinct phononic behavior for BAWs, SAWs, or Lamb waves propagating parallel or perpendicular to the periodicity. In practice, 1D bulk PnCs are superlattices (SLs), i.e., stacks of periodically alternating layers of different elastic impedances .[140–144] 1D PnCs are straightforward systems, which can host both phononic and photonic band gaps. The first direct measurement of the hypersonic phononic band gap in SiO_2/PMMA SLs was reported by Gomopoulos et al.[145]. The Brillouin light scattering (BLS) results revealed that the BG in such PnCs could be altered through the porosity of SiO_2 layers. The lattice imperfections, defects, or aperiodicity were investigated experimentally in terms of new phononic effects. The defects were investigated by probing the acoustic transmission[146] and dispersion relation (BLS)[144]. Going further, the aperiodic (quasiperiodic) 1D Fibonacci SLs [Fig. 4 (h)] were studied employing acoustic transmission[122] and femtosecond pump-probe spectroscopies[143]. In this case, the aperiodic structures were found as better acoustic filters than their ordered counterparts. In the case of the lattice disorder, acoustic Anderson localization was predicted theoretically for GaAs/AlAs SLs .[147] The propagation of SAWs in surfaces periodically corrugated in one dimension was theoretically studied already in the 70s. The recent experimental realizations of hypersonic 1D SAW PnCs were examined by BLS and pump-probe experiments.[123,126] Figure 4 (i) displays SEM image of PnCs made out of rectangular-like periodic grooves made on the (001) surface of crystalline silicon.[123] This system revealed hypersound filtering due to BG in the direction perpendicular to the grooves, while along the grooves, it worked as a waveguide for Lamb waves confined in the stripes. Recently, 1D gourd-shape PnC tethers showed reduced anchor losses and improved quality factor for Lamb wave resonators in the GHz range. This single-chip system can be potentially explored for applications for wireless communication devices.[148]

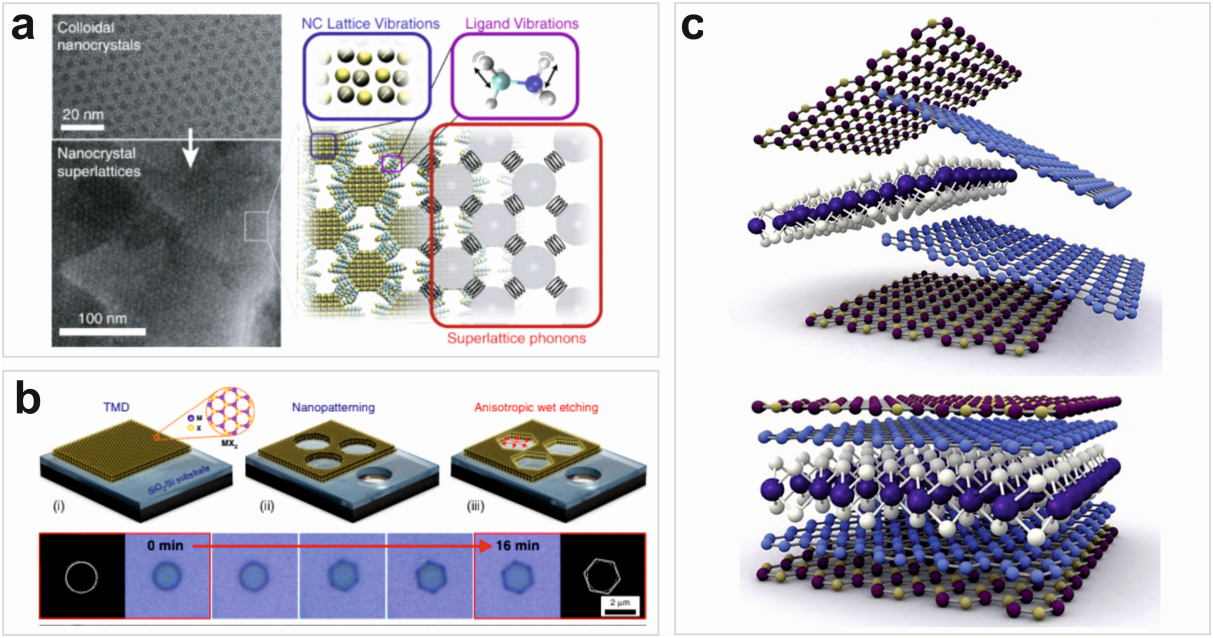

FIG. 5. Novel materials for nanophononics. Colloidal crystals made of ultrasmall semiconducting nanocrystals linked with polymeric ligands.[137] (b) Nanopattering and wet etching of supported TMDCs thin films.[138] (c) Illustration of 1D heterostructures made of vdW layered materials.[139] Figures (a-c) are reproduced with permissions from Refs. 137–139 and copyright obtained from 2019 Springer Nature, 2020 Springer Nature, and 2016 AAAS Publishing, respectively.

B. Metamaterials made of low-dimensional nanostructures

The PnCs mentioned so far have their band gaps centered around 1-20 GHz. To achieve higher frequencies (∼100 GHz to 1 THz) the PnCs need to have smaller feature sizes, i.e., in the order of tens to few nanometers. This downscaling implies a major challenge for standard nanofabrication techniques. Potentially, smaller PnCs can be assembled by low-dimensional materials like nanoclusters or quantum-dots (0D), nanotubes or nanorods (1D) and graphene-like materials (2D).

0D building blocks for nanodevices (e.g., quantum dots of chalcogenides and perovskites) have been widely studied due to their potential applications in optoelectronic devices, light-emitting diodes, photodetectors, and solar cells.[149,150] Notably, 0D structures of chalcogenides like CdSe, CdS and PbS can self-assemble and form CCs.[137,151–154] The available literature is comparably extensive for colloids based on perovskites such as mixed-halide nanocrystals,[155] or organometal halide perovskites.[156] More information on semiconducting colloids can be found in previous reviews.[149,150,157] Such systems have already been considered for the construction of photonic crystals.[156,158] In comparison with photonics, the application of 0D semiconductors in phononic devices is limited. However, acoustic phonons and various other structural motions affect the electronic states and optical properties of chalcogenide and perovskite colloids and crystals.[159–163] Regarding extrinsic interactions, scattering of SAWs on supported quantum dots can modify their energy levels.[164] This interaction enables various interesting applications at the interface of phononics and optoelectronics, which involve control of semiconducting quantum dots with SAW devices.[165] Based on all the above, CCs made of 0D semiconducting nanostructures represent a new type of phononic metamaterial that deserves additional experimental investigations —see Fig. 5 (a) and the work of Yazdani et al.[137]

While the formation of CCs relies on the spontaneous behavior of 0D nanostructures (self-assembly), the synthesis of metamaterials out of 2D nanostructures can be more controlled. For instance, 2D PnCs can be fabricated by pattering transition metal di-chalcogenides (TMDCs) —see Fig. 5 (b) and the work of Munkhbat et al.[138] These graphene-like materials have attracted considerable attention over the last decade. Thus their mechanical, electronic, thermal, and optical properties are relatively well-known. TMDCs are also termed layered materials and van der Waals (vdW) materials. This means that their atoms are arranged in 2D layers held together by weak vdW bonds. Hence, various TMDCs, like MoS_2, $MoSe_2$ and WS_2, can be prepared in the form of ultrathin membranes.[166–170] The thickness of TMDCs can be as small as one layer using liquid[171] or mechanical[172] exfoliation from the bulk. In order to employ these materials as 2D PnCs, it is necessary to introduce periodic patterns. This can be achieved in various ways. For instance, Yun et al. created nanopatterns on supported MoS_2 by block copolymer lithography.[173] Munkhbat et al.[138] created TMDC metamaterials with a three-step process: i) transfer of mechanically exfoliated TMDCs on a desired substrate, ii) use of nanopatterning techniques like EBL, RIE or focused ion beam (FIB) and iii) anisotropic wet etching [Fig. 5 (b)]. This approach offers perforated TMDCs (like WS_2, MoS_2, and $MoSe_2$) with nearly atomi-

cally sharp zig-zag edges.[138] Moreover, FIB can be used to introduce single-atom defects/holes in free-standing monolayer TMDCs.[174] Kozubek et al.[175] used highly charged ions to drill well-defined pores in free-standing MoS_2 with sizes of several nanometers. Irradiation with He^+ has also been used to perforate free-standing TMDCs (MoS_2).[176] Additionally, linear patterning of TMDCs[173] can be used to prepare metamaterials with grooves. Zhang et al. moved a step further and demonstrated atomically thin photonic crystals made of square arrays of holes on free-standing WS_2.[170] Additional flexibility in the design of TMDC metamaterials can be achieved with nanopatterning of vdW heterostructures as the ones illustrated in Figure 5 (c).[139] In this case, the system will act as a 1D superlattice normal to the layers and as a 2D metamaterial parallel to them.

The use of low-dimensional nanomaterials to construct novel PnCs will introduce new challenges for experimental and theoretical studies in phononics. Widely adopted experimental techniques like BLS, pump-probe measurements, Raman, X-ray, and neutron scattering will have to deal with poor signal-to-noise ratio due to the small dimensions of the samples. Spectroscopic techniques based on inelastic light scattering (for instance, spontaneous BLS) will be limited by the opaqueness of the samples and the high frequencies (small thermal occupations) of acoustic phonons. Moreover, the confined acoustic phonons are expected to be affected by various microscopic couplings that need to be measured. For instance, the use of metallic, semiconducting, or magnetic nanomaterials will enable couplings of acoustic phonons with plasmons, electron-hole pairs, and magnons. We believe that many of these challenges can be addressed with pumped-BLS, a recently developed hybrid technique that combines ultrafast photoexcitation of confined acoustic phonons with BLS detection in frequency-domain.[177] This technique offers hundred-fold amplification of BLS signal from semiconducting nanomembranes and reveals interactions of acoustic phonons with charge carriers —see Vasileiadis et al. for further details.[177]

IV. OPTOMECHANICAL CRYSTALS

The commensurated wavelength of GHz phonons and telecommunications electromagnetic radiation in the most important platforms for microelectronics and photonics, as silicon and silicon nitride, allowed the demonstration of optomechanical (OM) coupling in micron size cavities.[178] Optomechanical coupling exploits co-localization of phonons and photons to maximize the energetic exchange between them, paving the way to manipulate phonon population until reaching average population below 1 in selected modes (Ground State cooling[179] – red detuned light excitation) and generation of amplified coherent phonon emission or phonon lasing[180] (blue detuned light excitation) for example. In the same kind of cavities, other schemes exploit optical free carrier generation and thermal dynamics to generate self-sustained amplified phonons at lower frequencies.[181]

Optomechanics is a huge research field with a plethora of promising applications in telecommunications and sensors (e.g. memories[182] and accelerometers[183]). It has a long term vision in quantum computation exploiting coherent phonon manipulation,[184] and in topological phonon propagation with OM as driving effect.[185] In this direction, plenty of efforts have been devoted to increasing phonon lifetime by shielding the structures from the sources of dephasing, first by a phonon band gap structure surrounding the OM cavities, after by selecting unit cells already providing its own bandgap (in 1D[186] [Fig. 6 (a)] and 2D[187]).

In particular, self-driven OM oscillators are ideal building blocks for exploring the collective dynamics of networks of coupled oscillators.[188,189] The observation, control, and exploitation of collective phenomena such as synchronization will find various additional applications, such as neuromorphic computational platforms, on-chip robust time keepers, and mass, gas, and force sensors with extremely low phase noise. Experimental observation of synchronization phenomena in pairs of coupled OM oscillators[190,191] has been already reported and scaling up the number of coupled oscillators would not substantially increasing the technological requirements.

We center now our attention to the capability of OM systems for ultrasensitive sensing of mechanical wave propagation using light (transduction), placing an optomechanical transfer gate, in the form of an integrated optomechanical cavity[192] or visualizing the movement of an antenna-like mechanical resonator coupled to propagating phonon modes, that can be simply done by analyzing the modulation of a reflected beam,[193] is essential to build circuit functionalities using phonons. This capability is particularly technologically relevant as it is currently being extended to bridge the transfer of information between microwave electrical and optical modulated signals in an energy efficient way. Hybrid systems, including piezoelectric and optomechanical system, report the highest yields in the GHz regime at modest power dissipations in the standard $LiNbO_3$ platform[194] [Fig. 6 (b)], what can cover a crucial demand of our information society: efficient transceivers for the huge data centers operating nowadays. In such systems, an incident microwave signal in an Interdigitated Transducer (IDT) is converted to a propagating phonon, guided and transform until scattering towards an OM cavity where an optical signal, previously injected in the circuit, is modulated by the signal. This process is bidirectional: a modulated optical signal injected in the circuit can excite mechanical motion in the OM cavity, that guided and transformed towards the IDT generates a microwave signal.

Those systems could become more compact if efficient GHz phonon generation replaces IDTs, in that sense, the first proof-of-concept experiment,[180] where GHz phonons are generated in an OM cavity, routed by phononic waveguides and transduced back to RF signal by another OM cavity, have been followed by studies to increase phonon lifetime, that is, minimizing phonon waveguide losses by exploiting phononic bandgap acoustic shielding,[195] engineering elastic strain[196] or using topologically protected edge states.[197]

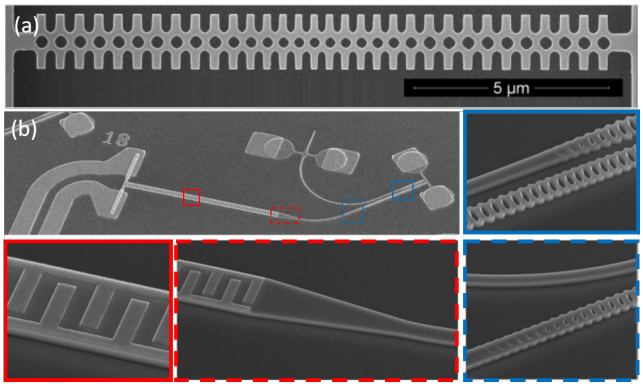

FIG. 6. Optomechanical crystals. (a) 1D OM crystal with full Phononic bandgap. Reproduced with permission from Ref. 181, copyrights obtained from 2015 Springer Nature. (b) Scanning electron micrographs (SEM) of one piezo-optomechanical transducer. Zoomed-in SEMs show the conversion region between microwave and mechanics (red) and between mechanics and optics (blue) from Ref. 191.

V. THERMAL TRANSPORT

Phonons are the primary heat carriers in solid dielectrics and semiconductors. According to Bose-Einstein statistics, at room temperature (RT), phonons of frequencies up to several THz are excited.[3,198] Notably, this broad-spectrum contributes to the transport of the vibrational energy and can be effectively tailored by the spatial nanoconfinement.[199–202] The recent remarkable progress in the field of the nanoscale thermal transport has proved that the breakdown of the Fourier's law, strong suppression of the phononic thermal conductivity, wave-like propagation of heat, observation of the second sound in solids at moderate temperatures, thermal cloaking, focusing and rectification, to name a few.[4,18] Nowadays, it is clear that confinement of thermal phonons at micro-and nanoscale offers fascinating features and challenges in their transfer to the mainstream technology applications. To explain the basic concept of nanoscale thermal engineering, we recall the kinetic theory, which defines the phononic thermal conductivity as $\kappa \propto C v_g \Lambda$.[200] Here, C is the heat capacity, v_g denotes the average group velocity, and Λ stands for the mean free path (MFP) of phonons. The latter parameter is an average distance traveled by a phonon between two scattering events, which can occur on impurities, imperfections, phonons (umklapp), electrons, and boundaries.[3,18,200] Notably, this much-simplified description allows for a good estimation of thermal conductivity for various materials. Furthermore, it points to phonon MFP and group velocity as being essential to alter the thermal conductivity. The research from the last decade has revealed that both of these quantities can be modified using PnCs with sub-micrometer feature size.[4,18,203–219] Indeed, shortening of the phonon MFP can result from imperfections between periodic motives and the matrix constituting PnCs. In this case, the interface roughness is comparable with the wavelength of thermal phonons. Thus, thermal phonons behave like particles that are diffusively scattered on the interfaces. As the phase is not preserved, this phenomenon is referred to as the incoherent effect.[18,220,221]

The second-order periodicity of PnCs alters the phonon dispersion relation, which implies reduced v_g, altered DOS, and under certain conditions, phononic bandgaps.[9,10,119,220] This approach utilizes the wave nature of phonons, and it requires both specular reflections from interfaces and MFPs of phonons (more rigorously phonon coherence length) that are at least a few times longer than the PnC periodicity. This phenomenon is referred to as the coherent effect in the literature, while PnCs are termed thermocrystals.[18,209] Unambiguous experimental evidence for the coherent heat conduction, thermal phonon localization, and crossover from coherent and incoherent regimes was demonstrated for 1D PnCs (superlattices). Notably, such phenomena to be observed at room temperature require structures of dense and atomically smooth interfaces.[212–214]

The dual, wave-particle nature of thermal phonons in 2D PnCs is a topic of ongoing widespread debate. Numerous works have reported reducing phononic heat conduction in membranes of periodic porosity with respect to the pristine membrane. The controversial issue that has arisen is the contribution of coherent effects near room temperature in PnCs with lattice parameter greater than 100 nm.[121,203,205,208,218,222,225,226] In this case, the relevant PnCs were made using electron beam lithography (EBL) and reactive ion etching (RIE) or focused ion beam (FIB) milling (see examples in Fig.7). Both approaches allow the fabrication of holes with roughness of few nanometers and amorphization in the best scenario.[125,203,208] To date, a real demonstration of the coherent effects was only possible at few Kelvin and sub-Kelvin temperatures for Si and Si_3N_4 PnCs, respectively. In these conditions, heat is carried via long MFP, GHz phonons of about micrometer wavelengths that are much larger than the surface roughness. On the other hand, in bulk Si at room temperature, MFPs span a broad range, and those longer than one μm contribute to 50% of the total thermal conductivity at room temperature. In general, this allows thermal phonons to travel over several lattice periods of PnCs and interfere, and thereby manifest wave-like nature. Accordingly, some of the prior works explained the suppression of κ as a combination of incoherent and non-negligible, coherent effects. Recent works, based on indirect and direct methods, have not confirmed those results. Namely, the disordered and aperiodic PnCs show the same thermal conductivity as their ordered counterparts [Fig. 7 (b)].[203] More directly, results obtained using BLS[119] and ASOPS[121] have confirmed modification of the phonon dispersion up to tens of GHz, what is relevant at very low temperatures, but negligible at RT. Furthermore, two-phonon Raman spectra [Fig. 7 (c)] that reflect phonon DOS proved no difference between spectra of PnCs and pristine membrane in the THz.[205] Even though the concept of the room temperature thermocrystal is doable, it can only be implemented in PnCs of the few-nanometer period and atomically smooth interfaces.[18]

Further development of PnCs dedicated to the management of thermal phonons can result from application-oriented directions such as thermal energy harvesting, extreme temperatures

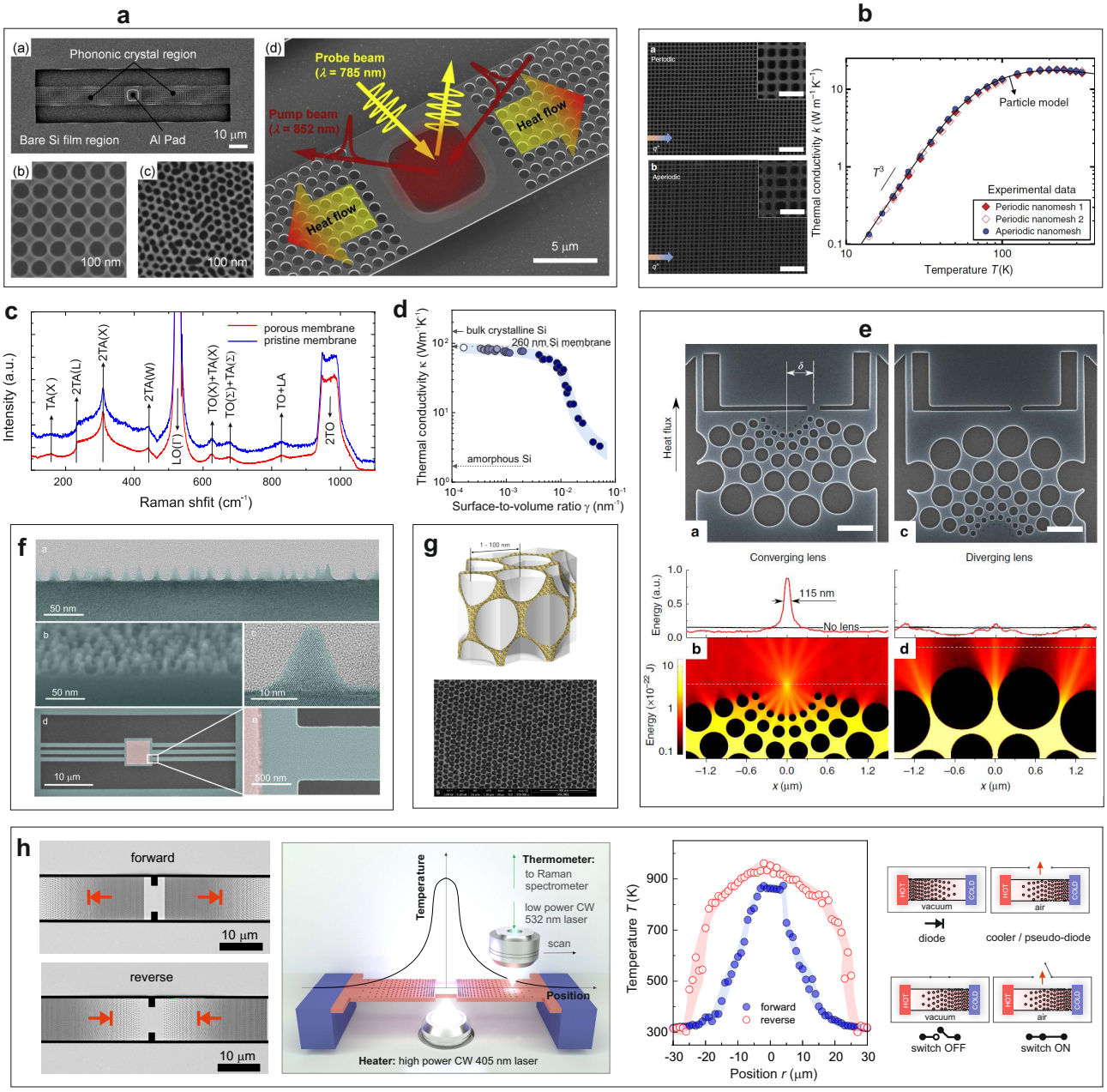

FIG. 7. (a) SEM images of the Si PnCs fabricated in a suspended architecture for thermal reflectance measurement.[215] (b) SEM image of a (left panel) periodic Si nanomesh with a period of 100 nm and (middle panel) an aperiodic Si nanomesh with the pitch varied from 80 to 120 nm. Scale bars are 200 nm (inset) and 600 nm (main). (right panel) Measured thermal conductivities of periodic and aperiodic nanomeshes as a function of temperature indicate the negligible role of the coherent effects.[203] (c) One- and two-phonon Raman spectra of pristine 250 nm membrane without and with pores obtained at room temperature. The critical points of the first Brillouin zone are identical for both samples.[205] (d) Thermal conductivity of porous membranes at 300 K as a function of the surface-to-volume ratio.[216] (e) SEM images of (left upper panel) converging and (right upper) diverging thermal lens samples with slits for heat dissipation. The scale bar is 1 μm. Monte Carlo simulations results of (bottom left) the formation of a hot spot in the focal point and (bottom right) dispersion of heat in the diverging lens.[222] (f) TEM and SEM images of 20 nm-high nanopillars fabricated on 50 nm-thick silicon membranes[223]. (g) A scheme and SEM image of a metalattice made of a closely spaced distribution of spherical voids in crystalline silicon.[224] (h) From left to right: SEM images of the thermal rectifiers in the forward and reverse configurations, schematic of the two-laser Raman thermometry experiment, temperature profiles of the test devices in the forward (solid purple circles) and reverse (red-outlined circles) configurations, schematics of possible devices based on the thermal rectifier.[216] The (a-h) are reproduced with permissions from Refs. 203, 215, 222–224 with copyrights obtained from 2020 Elsevier Ltd, 2017 Springer Nature, 2017 Springer Nature,2020 Elsevier Ltd, 2017 Springer Nature, 2020 American Chemical Society.

and gradients, effective heat dissipation, geometry engineering towards ray-like heat transfer, the synergetic combination of conduction with convection or radiation, and thermal rectification, new materials as platforms for PnCs, and materials hosting other elementary excitations being, in addition to phonons, heat carriers.

The reduced thermal conductivity in 2D porous PnCs holds great potential for applications in thermal energy harvesting, sensing, and heat flow management.[227] In particular, crystalline porous Si membranes can be used to realize Slack's "phonon glass – electron crystal", i.e., hypothetical material of maximized thermoelectric (TE) figure of merit ZT.[228] Hence, the perforation leading to κ as low as the amorphous limit has to maintain the electronic properties. The latter can be further engineered by doping towards an optimized electronic power factor. Yet, recent works have reported TE generators made of porous Si membranes with $ZT << 1$ around RT, which is significantly less than what is offered by conventional materials.[207,210,211,227] However, Si PnCs are CMOS-compatible and therefore can be easily implemented in mainstream technology. For instance, the upcoming market of the Internet of Things can benefit from cheap and robust self-powered units or sensors based on such structures.

Furthermore, silicon and silicon on insulator (SOI) technologies are the most mature for producing micro and nanoscale devices dedicated to high-temperature applications.[229] The high temperature is a considerable value market for thermal sensing and energy harvesting in the automotive, airspace industry, space exploration, metallurgy, and conventional energy production.[230] Besides a few recent works[205,216], thermal properties of PnCs at temperatures exceeding 500 K remain primarily unexplored area due to experimental challenges. Thus, novel tools based on, most likely, contactless approaches are needed [Fig. 7 (h)].

As follows from theoretical works, local resonances can be an alternative approach for thermal phonon blocking in 2D PnCs. In this concept, PnCs consist of a 2D array of pillars deposited on the membrane. In this structure, the hybridization between localized modes in pillars and propagating modes in the membrane results in sub- and super-wavelength bandgaps that are immune to the PnC lattice's imperfections.[231,232] Besides that, typical phononic effects can appear due to the periodic arrangement of pillars. Consequently, phonon group velocity, DOS, and hence thermal conductivity can be tuned (in addition to lattice spacing) by the characteristic sizes and mass of the pillar. The modification of the dispersion in these structures was confirmed experimentally for GHz phonons employing BLS. However, the importance of coherent effects on the thermal conductivity has been recently questioned based on the experimental results obtained in the 4-300 K range.[223,233]

Recently, Anufrief and Nomura have proposed a concept of ray phononics utilizing ballistic heat transport in porous membranes.[222] Such materials are envisioned for ray-like heat flow management in nanostructures regardless of their surface imperfections and foremost possible at room temperature. The proof-of-concept experiments have proved such features as thermal phonon guiding, emission, and focusing [Fig. 7 (e)].

Needless to say, that wealth of new features resulting from the phonon confinement go hand in hand with technological challenges. Indeed, the progress of miniaturization and electronic devices' performance in the last two decades has encountered a bottleneck related to the efficient removal of the produced heat. Thus, both size-reduced thermal conductivity and volume can lead to overheating and eventually damage of nanoscale components. Porous membranes can be an effective and low-cost solution to this problem, which utilizes passive cooling units via air convection. Simultaneously, the vast majority of previous thermal studies of porous membranes were performed in vacuum conditions. However, convection in porous membranes deserves more attention regarding the real conditions for their operation and possible application in passive cooling. As follows from recent experiments, the heat dissipation via combined convection and conduction can be optimized via the structure surface-to-volume [Fig. 7 (d)] ratio.[205,216]

The enhancement of the heat dissipation in nanostructured membranes (depending on the material) can be seen in less obvious elementary excitations such as surface phonon-polaritons (SPhPs), magnons, or plasmons. Wu et al. have demonstrated that the thermal conductivity of sub-50 nm thick Si_3N_4 membranes doubles as the temperature increases from 300 to 800 K due to SPhPs.[234] In perspective, new architectures of PnCs can primarily benefit from a synergetic combination of dielectric or semiconducting membranes with metallic and magnetic layers or nanostructured motives. In particular, the emerging fields of spin caloritronics[235,236] and the intersection between plasmonics and phononics[237] are attractive directions for further developing the nanoscale thermal transport in periodic structures. Another and quite natural step forward can be the fabrication of macroscale 3D PnCs for thermal flow management using self-assembled colloidal crystals[238,239], metalattices[224], or atomic quality hybrid (organic-inorganic) Bragg stacks[21]. Notably, the aim of the latter materials is, contrary to the majority of PnCs, to enhance the thermal conductivity to remove process heat in organic electronics preserving transparency and flexibility.

One of phononics' main ambitions is to use heat as the information carrier and develop thermal analogs of diodes, transistors, and electronics switches.[4,240–242] The fundamental requirements for a thermal diode (or rectifier) can be satisfied by porous membranes. Namely, they offer temperature dependence of the thermal conductivity (non-linearity) and space dependence (spatial asymmetry) of the thermal conductivity. Practical realization of thermal rectification was reported for perforated graphene (26% efficiency at RT)[243] and recently for Si membrane. The latter structure (14% efficiency) is dedicated to operation at high temperatures up to 1000 K and can also be utilized as a thermal switch or optimized convective cooler [Fig. 7 (h)].[216]

Overall, the future of PnCs requires new platforms that can host phononic effects and introduce new physical and chemical features. From this perspective, an excellent opportunity is the wealth of van der Waals materials, and their heterostructures offer unique, highly anisotropic, and

size-dependent electronic, optical, thermal, and mechanical properties.[139,244–246] Nevertheless, this requires a significant advancement in the fabrication of robust large area samples and experimental tools development.

VI. TOPOLOGICAL PHONONICS

A. From symmetry to topology

Up to this point, we discussed phononic metamaterials whose properties depend solely on the crystal symmetry and are strongly affected by defects and disorder. The relevant transport phenomena are characterized by losses, left-right symmetry (parity, P) and time-reversal symmetry (T). This section presents a novel type of metamaterials, termed topological phononics, which offers robustness to disorder, one-way propagation of phonons (broken P or T symmetry) and transport without losses. In most cases, the different phases of condensed matter are adequately characterized by distinct symmetries, and a symmetry-related order parameter describes the passage from one phase to another. However, it is possible to observe phases of matter that do not depend on the sample's size, shape, composition, and impurities. The unique identification of such phases requires some topologically invariant property, meaning a property that remains constant under continuous transformations.

Topology has first entered the realm of experimental, condensed matter physics in 1980 with the discovery of the Quantum Hall Effect (QHE) by Von Klitzing et al.[247] The QHE is the quantized Hall conductance of a two-dimensional (2D) electron gas in a strong magnetic field and at low temperature. Subsequent studies revealed several more types of topological phenomena for electrons and spins in crystals. For instance, in the Quantum Spin Hall Effect[248] (QSHE) the spin Hall conductance of 2D crystals is quantized due to spin-orbit coupling without a magnetic field. Another relevant electronic degree of freedom is the valley, i.e., the bands extreme that the electrons occupy, which gives rise to the Quantum Valley Hall Effect[249,250] (QVHE). The observation of topological phenomena in three-dimensional (3D) crystals gave rise to the so-called topological insulators.[251,252] In these materials, the topology of the bulk states is distinct from that of the surrounding vacuum, leading to the creation of unique, conductive surface states. Dirac semimetals are insulating in the 3D bulk and have 2D surface states with Dirac cone dispersion.[252] Weyl semimetals have topologically protected Dirac cones in the 3D bulk, and surface states with unique, arc-shaped dispersion.[253–256] Additionally, Floquet topological insulators have conductive surface states due to external, periodic, temporal perturbations[257,258] From the perspective of basic science, topological condensed matter systems can be used to perform tabletop experimental studies of exotic particles that remain unobserved in nature, like magnetic monopoles,[259–261] as well as Dirac and Weyl fermions.[252]

The first experimental realization of topological phenomena for classical waves and metamaterials occurred in 2009 by Z. Wang et al.[262] who demonstrated a topological photonic metamaterial operating in GHz frequencies (microwave radiation). The readers can find more information about topological photonics in the review articles of Lu et al.[263] and Ozawa et al.[264] The first topological acoustic metamaterial was realized by Fleury et al.[265] in 2014. This acoustic crystal consisted of ring resonators, where left-handed and right-handed modes were initially degenerate. The degeneracy was then removed with a biasing airflow, leading to one-way transport of sound. Topological phononics have been discussed in a number of previous review articles.[266–268] Here, after a short introduction, we emphasize the novel topics of 1D topological phononics, higher-order topological insulators, and programmable topological phononics. Next, we discuss how the various macroscopic designs can be re-adapted for topological nanophononics in the gigahertz (GHz) frequency range. We conclude this section with a proposal on studying low-dimensional, topological nanophononics in the GHz range, using a recently developed combination of Brillouin spectroscopy and ultrafast photoexcitation.

B. Topology for condensed matter physics

In the band structure theory of insulators, topology is used to examine if one insulator can be smoothly transformed into another. If this is not the case then a topological phase transition must occur at their interface leading to the creation of spatially confined conductive states. As an example to describe Chern insulators, the starting point for defining the topologically invariant property is the Berry phase[269,270] (γ), which is used to describe the change of a quantum state with respect to some variable (X(t)) of the system's Hamiltonian that changes slowly with time (adiabatically). In condensed matter physics, the X is the wavenumber k (of electrons, phonons, or other quasiparticles), and the adiabatic change is a motion in reciprocal space. If this motion follows a closed path, and for a 2D crystal, the Berry phase is given by:

$$\gamma = \oint \boldsymbol{A}(\boldsymbol{k}) \cdot d\boldsymbol{k}. \tag{1}$$

The $\boldsymbol{A} = i\langle \phi_{nk} | \nabla_k | \phi_{nk} \rangle$ and it is called the Berry connection or the Berry potential[269–271] (in analogy to the vector potential of electrodynamics). The function ϕ_{nk} is taken from the Bloch theorem: $\Psi_{nk}(\boldsymbol{r}) = e^{i\boldsymbol{k}\cdot\boldsymbol{r}}\phi_{nk}(\boldsymbol{r})$. Next, the Berry phase can be re-written as $\gamma = 2\pi C$, where C is the Chern number,[270] which is the topologically invariant property of the Chern insulators according to the Thouless–Kohmoto–Nightingale–den Nijs (TKNN) theory.[272] Using the Stokes theorem and relationship 1, the Chern number is given by:

$$C = \frac{1}{2\pi} \iint_{BZ} \nabla \times \boldsymbol{A}\, d^2\boldsymbol{k}. \tag{2}$$

The integration is over the entire Brillouin zone (BZ). Due to periodic boundary conditions, the integration area is also called the Brillouin torus.[271] The vector field $\nabla \times \boldsymbol{A}$ is called the Berry curvature.[269–271] The integral of relationship 2 is the flux of the Berry curvature field through the Brillouin torus.

To achieve interesting topological properties (e.g. topological surface states, one-way transport and robustness to disorder), the Brillouin torus must contain a source of the Berry curvature field giving a non-zero Chern number. For plane waves or vacuum, the ϕ_{nk} is constant and $C = 0$. Thus, if the bulk has insulating states with $C \neq 0$, a topological phase transition occurs at the surface with the emergence of gapless surface states. Similarly, confined gapless states appear at the interface between topologically distinct insulators (different Chern numbers). The latter topological phase transitions can be viewed as a band inversion — for instance, see the schematic illustration from Z. Zhang et al.[273] in Fig. 8 (a).

C. Macroscopic topological phononics in various dimensions

In one-dimensional (1D) phononic crystals, topological edge states are localized oscillations without transport. Topological properties in 1D can arise due to some spatial modulation, e.g., of losses[274] [Fig. 8(b)]. The topological acoustic crystal of Gao et al.[274] [8 (c) left] has a bulk spectrum that is depleted at 2,150 Hz [Fig. 8 (c) center], while the edges' spectrum has a maximum at the same frequency [Fig. 8 (c) right]. Additionally, 1D phononic crystals have been shown to possess interfacial states[275] (states between topologically distinct insulators) and Weyl particle physics.[276]

Since most of the relevant topological physics requires spin-dependent phenomena, several studies of acoustics explored acoustic pseudo-spin,[281–285] acoustic QSHE,[286] and acoustic analogues of spin-multipoles.[287] Pseudo-spin-dependent transport was shown to be robust and to possess transmission without backscattering — see for instance Refs. 285 and 286. Pseudo-spin states can be formed in the presence of double Dirac cones. Double Dirac cones have been introduced in various ways, e.g., with zone-folding in a triangular lattice of rods,[288] or with 2D arrays of Helmholtz resonators,[289] or with local resonance states.[290] Two-fold Dirac point degeneracy appears for graphene-like phononic crystals[291] and more complicated structures, like 2D kagome[292] and Kekulé lattices.[293] In the case of 2D square lattices, the Dirac cones can appear away from the high-symmetry points of the band-structure[294,295] — a phenomenon described as accidental degeneracy. Moreover, 2D sonic crystals have been used to realize acoustic Floquet topological insulators.[281,284] Notably, topological properties in 2D (or quasi-2D) systems can also arise from water surface waves.[296–299]

Regarding 3D systems, He et al.[300] showed that topological valley states can emerge at the interface of two crystals with opposite valley Chern numbers. Other studies using 3D metamaterials have demonstrated acoustic analogues of Weyl and Dirac semimetals,[301] negative refraction,[302] acoustic quadrupole[303] and octupole[304,305] topological insulators, and topological properties in granular metamaterials.[306] Moreover, Peng et al.[307] have demonstrated 3D Floquet insulators, using a periodic, spatio-temporal modulation in a sonic crystal. Very recently, Fu et al.[308] have studied sound vortices in 3D cylindrical waveguides and demonstrated diffraction of sound that depends on the value of the topological charge. In relevance with sound vortices, helical-acoustic metamaterials can be used for dispersion-free deceleration of sound[309] and can potentially be useful for topological acoustic metamaterials.

A special type of topological materials termed higher-order topological insulators,[277,292,310] support edge states that are two or more dimensions lower than the bulk states. For instance, in a third-order topological insulator, some of the states are confined on the corners (0D) of a 3D crystal.[310] Zhang et al.[277] have demonstrated a second-order, 2D topological insulator, whose structure and properties are illustrated in Figs. 8 (d-i). Its unit cell [8 (e)] consists of four drilled holes; the yellow and the blue parts are the rigid materials and the air, respectively. This 2D crystal is split into two regions with trivial and nontrivial topological properties [Fig. 8 (f)] by varying the ratio of the distance between holes R over the lattice constant a. Using finite element method (FEM), the authors have visualized the pressure distributions in the trivial and nontrivial regions and illustrated a band inversion from p- to s-like "conduction" states and from s- to p-like "valence" states [Fig. 8 (g)]. The vibrational density of states [Fig. 8 (h)], which was recorded using a loudspeaker and a microphone, shows 2D bulk states, 1D edge states, and 0D corner states, thus proving the second-order character of this topological acoustic crystal transport.

D. Programmable topological phononics and applications

Macroscopic metamaterials offer the possibility of real-time and on-demand structural changes. Thus, it is possible to control the topological properties in versatile, uncomplicated ways, and to construct smart devices for sound manipulation. For example, Zhang et al.[277] generated programmable patterns of acoustic fields [Fig. 8 (i)]. Xia et al.[278] have developed honeycomb-lattice sonic crystals that can be reconfigured with air cylinders [Fig. 8 (j) top]. Using this design, the authors managed to control the path followed by the edge states between two topologically distinct phases [Fig. 8 (j) bottom]. Tian et al.[279] have realized a tunable, sonic honeycomb lattice by infiltrating liquid in its holes [Fig. 8 (k) top], which was again used to control the path of edge states [Fig. 8 (k) bottom]. Zhang et al.[273] constructed a hexagonal array of rotatable, three-legged elements [Fig. 8 (l) top] that could be used as a phononic delay line [Fig. 8 (l) bottom]. A prominent application of topological manipulation of sound is the construction of directional loudspeakers and microphones[280,311] [Fig. 8 (m)]. Regarding prospects, another exciting class of devices (which have not been experimentally realized at the moment for phononics) are one-way, topological, beam splitters.[312–315]

Moreover, topological phononics support edge states with one-way transport[281,286,316–318] and, thus, they can be used as phononic diodes[216,319,320] or waveguides[321]. It would then be interesting to use programmable topological phononics in order to construct switches and gates for phonons that

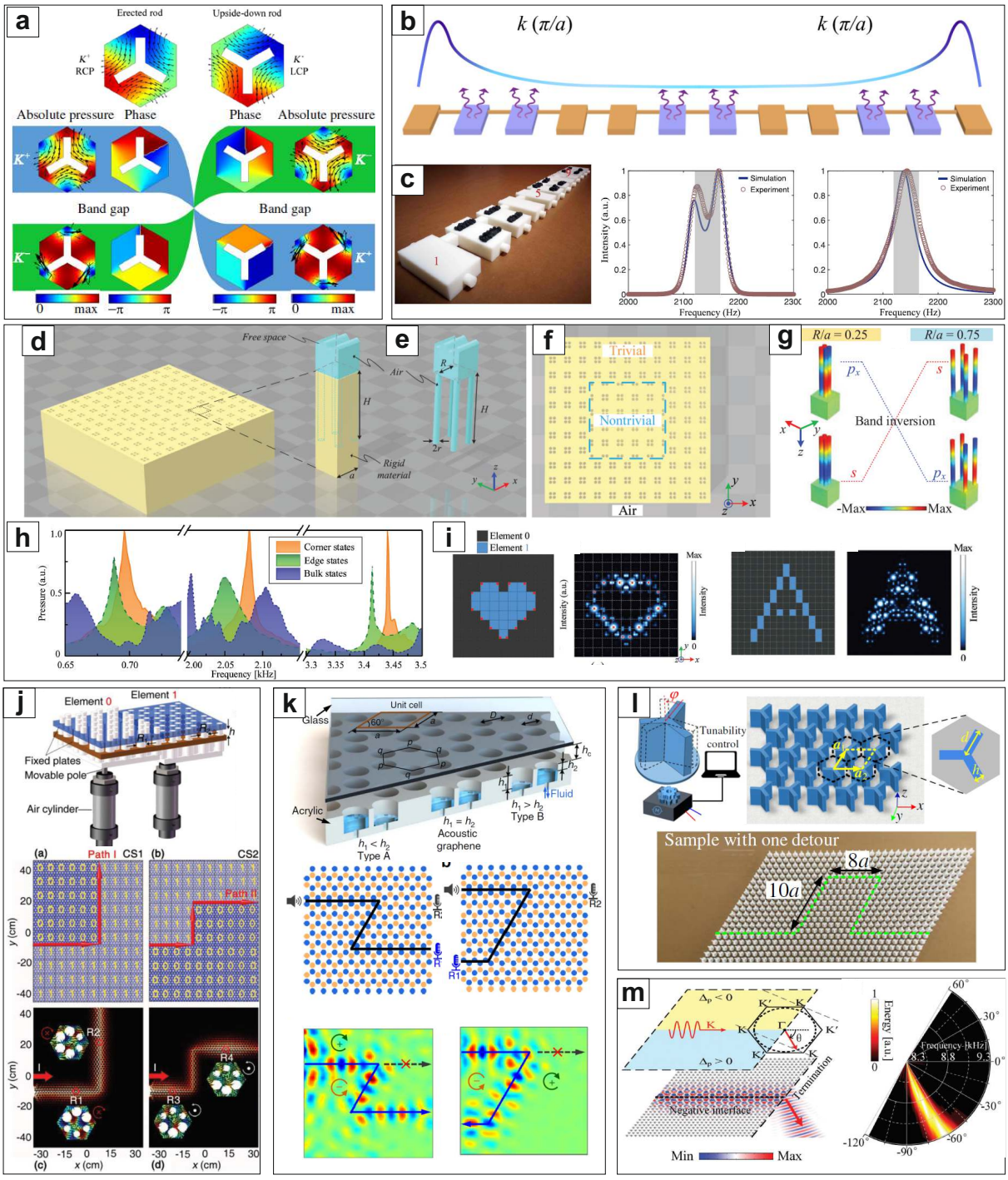

FIG. 8. Topological acoustics in 1D and 2D: (a) Rotatable three-legged-rods used to create spinning acoustic fields (up) and a topological phase transition of these acoustic pseudospin states (down) from Zhang et al.[273] Copyrights obtained from 2018 American Physical Society. (b) Schematic of a 1D acoustic lattice with topological properties arising from spatial modulation of losses. Copyrights obtained from 2020 American Physical Society. (c) Image of the sample (left), acoustic resonances inside (center) and at the edges (right) of a structure studied by Gao et al.[274] (d) Design of a second-order, 2D topological insulator,[277] (e) its unit cell, (f) illustration of the boundaries between trivial and nontrivial topological regions, (g) diagram of the topological phase transition through band inversion, (h) VDOS for corner, edge and bulk states and (i) programmable patterns of acoustic fields. Tunable topological acoustics and applications: (j) Programmable 2D topological acoustic crystal controlled by pressurized air,[278] (k) tunable 2D topological acoustic crystal using liquid infiltration,[279] (l) acoustic delay line based on a tunable topological acoustic crystal,[273] (m) directional emission of sound using topological acoustics.[280] The (a)-(m) are reproduced with permissions from Refs. 273, 274, 277–280 and copyrights obtained from 2018 American Physical Society, 2020 American Physical Society, 2020 Springer Nature.

mimic electronic circuits.[87,88,322] Another interesting way for tuning the properties of topological phononic crystals is to take advantage of the physics of Floquet topological insulators, whose properties can be controlled by external fields, lasers, microwaves or other types of radiation.[323] Finally, tunable topological acoustics can make use of soft, deformable materials.[324]

E. Topological gigahertz nanophononics

The topological phononic crystals mentioned so far have macroscopic dimensions, resulting in sound waves in the kHz to MHz frequency range. One of the most promising application of phononics is their use in wireless devices, where they mediate signal processing of microwaves. For such applications, the phononic structures need to operate in the GHz range. The growing demand for signal processing at higher operational frequencies (5G wireless networks and beyond), and the vast progress of THz light technologies, will likely require phononic devices with higher operational frequencies. Higher operational frequencies can be achieved by spatial confinement of the phononic structures in the sub-μm to nm lengthscales (nanophononics).

Topological GHz nanophononics can be 1D systems like coupled nanocavity arrays.[325] These 1D systems are GaAs/AlAs superlattices with band-inversion at the interface, while the probing technique can be in frequency- (Raman[326]) or time-domain (ASOPS[327]). Regarding 2D systems, several interesting, macroscopic crystals (e.g., hosting topological acoustic polaritons[328]) can be scaled down to the sub-micrometer scale using lithographic techniques.[8,125,202] Based on several theoretical proposals, experiments, and simulations, a good design for topological nanophononics is pillared phononic crystals.[329–333]

Classical, macroscopic metamaterials can be precisely engineered in terms of their size, shape, and dimensionality. Thus, they can be used to evaluate the various designs and decide which of these can be transferred to the sub-micrometer lengthscale and GHz frequency range. For macroscopic 2D topological acoustics (see the work of Zhang et al.[277]) the experiments require sample-preparation by 3D printing, a loudspeaker to emit sonic waves and a microphone to detect the edge- and corner-states. For nanophononics, the 3D printing technology can be replaced by lithographic techniques.[125]

Generation of coherent acoustic phonons can be carried out with ultrashort laser pulses — see for instance Arregui et al.[327] The laser pulses generate coherent acoustic phonons through the thermoelastic effect and the displacement potential mechanism.[334] The probing of topological phonons in 2D PnCs can be potentially performed by micro-BLS, which has the ability to map the vibrational density of states and the band structure[335] as well as the direction of phonons[177] (asymmetric Stokes/anti-Stokes intensities) with micrometer spatial resolution. Finally, a practical way of tuning the crystal properties might come from heterostructures of hard semiconductors and soft, polymeric structures. In such heterostructures, it will be possible to deform the soft matter part with an externally applied strain, and therefore to tune topological phase transitions at the interface.[324] In this case, the additional usefulness of BLS is that it can measure directly and accurately the local strain, which causes flexural Lamb waves of zero momentum to have non zero frequencies.[336,337]

VII. SUMMARY

Research on PnCs is a relatively mature field that is more than 20 years old. The transition from research to the industry can be achieved for two types of PnCs: macroscopic sub-GHz PnCs for vibrational isolation and microscopic, hypersonic PnCs for MEMS and telecommunication. The design of PnCs can make use of various computational techniques like finite element methods,[338,339] acoustic transfer matrix calculations,[340] genetic algorithms,[341] topological optimization[342,343] and machine-learning.[60,344] These computational methods provide efficient but complex architectures, which can now be realized with 3D printing technologies, sophisticated machining, molding and casting for macroscopic PnCs, and bottom-up or top-down synthesis for microscopic PnCs – see the review article of Choi et al.[345]

Macroscopic PnCs with band gaps at audible frequencies,[311,341,343,346–353] and various acoustic metamaterials[354–356] can be used for sound insulation of buildings, vehicles and machinery. Moreover, macroscopic PnCs with non-trivial topological properties can be used to construct loudspeakers and microphones that control the direction[280,311] and timing[273] of sonic signals. Additionally, PnCs have promising applications for ultrasonic imaging for biomedical applications (section 2). Research on PnCs can even be useful for civil engineering and urban design. For instance, strategic planting of trees is the ultimate green method for protection against sound pollution[357] and seismic waves.[33–35] Protection from seismic waves can also be achieved with artificial, periodic structures called seismic metamaterials.[28] Similarly to seismic waves, PnCs, and metamaterials that control water waves can be used for coastal engineering[358] and to amplify energy harvesting from ocean waves.[359]

Higher operational frequencies for phononic devices can be achieved through spatial confinement and nanostructuring. Thus, hypersonic PnCs have potential applications for signal processing applications at 5G frequencies and beyond. Apart from higher operational frequencies, PnCs for telecommunications need to maintain high-quality factors (minimize dissipation), which is one of the main advantages of phononic devices compared to electronic circuits.[11] The most critical missing component is a reliable source of coherent phonons that can operate at high frequencies (»10 GHz). Likely, the development of coherent phonon sources at high frequencies can be facilitated by research on optomechanics (section 4). So far, PnCs were mostly based on semi-transparent, insulating materials (e.g., SiO_2 and polymers like PS) and well-known semiconductors with 3D crystal structures like Si. The need for further miniaturization of phononic devices

might be covered by novel, low-dimensional, semiconducting nanomaterials (Fig. 5). For instance, ultra-small 0D nanoclusters can self-assemble into colloidal crystals, and vdW layered materials can be used to construct ultrathin, crystalline metamaterials (section 3). However, the use of such novel nanomaterials will likely require a deeper understanding of microscopic interactions and dissipation processes for acoustic phonons. For instance, the use of metallic, semiconducting, and magnetic nanomaterials will require studies on the coupling of acoustic phonons with plasmons, excitons, and magnons, respectively. Additionally, metamaterials made of low-dimensional semiconductors can also be interesting in view of thermoelectrics (discussed in section 5). Tunable hypersonic PnCs can result from liquid-solid or organic-inorganic heterostructures (sections 3 and 6), which will be controlled by infiltration or deformation, respectively. The waveguiding of phonons (for instance, in a delay line) can be achieved using PnCs with band gaps and topological edge states (section 6). Thus, we consider that research in topological phononics will gradually move to high-order 2D topological nanophononics at gigahertz frequencies.

ACKNOWLEDGEMENTS

This project has received funding from the European Union's Horizon 2020 research and innovation programme, the Foundation for Polish Science (POIR.04.04.00-00-5D1B/18) and the Polish National Science Centre (UMO-2018/31/D/ST3/03882).

DATA AVAILABILITY

Data sharing is not applicable to this article as no new data were created or analyzed in this study.

REFERENCES

[1] I. I. Frenkel, *Wave mechanics; elementary theory,* (Clarendon Press) OCLC: 1477670.

[2] I. Tamm, "Über die quantentheorie der molekularen lichtzerstreuung in festen körpern," **60**, 345–363.

[3] J. M. Ziman, *Electrons and Phonons: The Theory of Transport Phenomena in Solids* (OUP Oxford) google-Books-ID: UtEy63pjngsC.

[4] M. Maldovan, "Sound and heat revolutions in phononics," **503**, 209–217 (), number: 7475 Reporter: Nature.

[5] L. D. Landau, L. P. Pitaevskii, A. M. Kosevich, and E. M. Lifshitz, *Theory of Elasticity: Volume 7*, 3rd ed. (Butterworth-Heinemann).

[6] B. A. Auld, *Acoustic fields and waves in solids*, 2nd ed. (R.E. Krieger) version Number: 2nd ed.

[7] P. A. Deymier, *Acoustic Metamaterials and Phononic Crystals* (Springer Science & Business Media) google-Books-ID: 8eg_AAAAQBAJ.

[8] Marianna Sledzinska, Bartlomiej Graczykowski, Jeremie Maire, Emigdio Chavez-Angel, Clivia M. Sotomayor Torres Francesc Alzina, "2d phononic crystals: Progress and prospects in hypersound and thermal transport engineering," , 1904434Reporter: Advanced Functional Materials.

[9] A. Khelif and A. Adibi, *Phononic Crystals: Fundamentals and Applications* (Springer) google-Books-ID: dNZECgAAQBAJ.

[10] V. Laude, *Phononic crystals: artificial crystals for sonic, acoustic, and elastic waves*, De Gruyter studies in mathematical physics No. Vol. 26 (De Gruyter) OCLC: 881822552.

[11] "Fundamentals and applications of acoustic metamaterials: From seismic to radio frequency,".

[12] Y. Pennec, J. O. Vasseur, B. Djafari-Rouhani, L. Dobrzyński, and P. A. Deymier, "Two-dimensional phononic crystals: Examples and applications," **65**, 229–291, number: 8 Reporter: Surface Science Reports.

[13] M. M. Sigalas and E. N. Economou, "Elastic and acoustic wave band structure," **158**, 377–382, number: 2 Reporter: Journal of Sound and Vibration.

[14] M. S. Kushwaha, P. Halevi, L. Dobrzynski, and B. Djafari-Rouhani, "Acoustic band structure of periodic elastic composites," **71**, 2022–2025, publisher: American Physical Society.

[15] D. A. Simons, "Reflection of rayleigh waves by strips, grooves, and periodic arrays of strips or grooves," **63**, 1292–1301, publisher: Acoustical Society of America.

[16] N. E. Glass, R. Loudon, and A. A. Maradudin, "Propagation of rayleigh surface waves across a large-amplitude grating," **24**, 6843–6861, number: 12 Reporter: Physical Review B.

[17] S. R. Seshadri, "Effect of periodic surface corrugation on the propagation of rayleigh waves," **65**, 687–694, publisher: Acoustical Society of America.

[18] M. Maldovan, "Phonon wave interference and thermal bandgap materials," **14**, 667–674 (), number: 7 Reporter: Nature Materials.

[19] R. Martínez-Sala, J. Sancho, J. V. Sánchez, V. Gómez, J. Llinares, and F. Meseguer, en"Sound attenuation by sculpture," Nature **378**, 241–241 (1995).

[20] Z. Liu, "Locally Resonant Sonic Materials," Science **289**, 1734–1736 (2000).

[21] Z. Wang, K. Rolle, T. Schilling, P. Hummel, A. Philipp, B. A. F. Kopera, A. M. Lechner, M. Retsch, J. Breu, and G. Fytas, "Tunable thermoelastic anisotropy in hybrid bragg stacks with extreme polymer confinement," **132**, 1302–1310 (), _eprint: https://onlinelibrary.wiley.com/doi/pdf/10.1002/ange.201911546.

[22] G. Ma and P. Sheng, en"Acoustic metamaterials: From local resonances to broad horizons," Science Advances **2**, e1501595 (2016).

[23] H. Ge, M. Yang, C. Ma, M.-H. Lu, Y.-F. Chen, N. Fang, and P. Sheng, en"Breaking the barriers: advances in acoustic functional materials," National Science Review **5**, 159–182 (2018).

[24] S. A. Cummer, J. Christensen, and A. Alù, en"Controlling sound with acoustic metamaterials," Nature Reviews Materials **1**, 16001 (2016).

[25] K. Bertoldi, V. Vitelli, J. Christensen, and M. van Hecke, en"Flexible mechanical metamaterials," Nature Reviews Materials **2**, 17066 (2017).

[26] A. Khelif and A. Adibi, eds., en*Phononic Crystals* (Springer New York, New York, NY, 2016).

[27] A. Palermo, S. Krödel, A. Marzani, and C. Daraio, en"Engineered metabarrier as shield from seismic surface waves," Scientific Reports **6**, 39356 (2016).

[28] S. Brûlé, E. Javelaud, S. Enoch, and S. Guenneau, en"Experiments on Seismic Metamaterials: Molding Surface Waves," Physical Review Letters **112**, 133901 (2014).

[29] S. Brûlé, S. Enoch, and S. Guenneau, en"Emergence of seismic metamaterials: Current state and future perspectives," Physics Letters A **384**, 126034 (2020).

[30] S. Brûlé, E. H. Javelaud, S. Enoch, and S. Guenneau, en"Flat lens effect on seismic waves propagation in the subsoil," Scientific Reports **7**, 18066 (2017).

[31] M. Miniaci, A. Krushynska, F. Bosia, and N. M. Pugno, "Large scale mechanical metamaterials as seismic shields," New Journal of Physics **18**, 083041 (2016).

[32] S. Krödel, N. Thomé, and C. Daraio, en"Wide band-gap seismic metastructures," Extreme Mechanics Letters **4**, 111–117 (2015).

[33] A. Colombi, P. Roux, S. Guenneau, P. Gueguen, and R. V. Craster, en"Forests as a natural seismic metamaterial: Rayleigh wave bandgaps induced by local resonances," Scientific Reports **6**, 19238 (2016).

[34] A. Maurel, J.-J. Marigo, K. Pham, and S. Guenneau, en"Conversion of Love waves in a forest of trees," Physical Review B **98**, 134311 (2018).

[35] J. Huang, Y. Liu, and Y. Li, en"Trees as large-scale natural phononic crystals: Simulation and experimental verification," International Soil and Water Conservation Research **7**, 196–202 (2019).

[36] A. Colombi, D. Colquitt, P. Roux, S. Guenneau, and R. V. Craster, en"A

seismic metamaterial: The resonant metawedge," Scientific Reports **6**, 27717 (2016).

[37]H. Meng, N. Bailey, Y. Chen, L. Wang, F. Ciampa, A. Fabro, D. Chronopoulos, and W. Elmadih, en"3D rainbow phononic crystals for extended vibration attenuation bands," Scientific Reports **10**, 18989 (2020).

[38]B. J. Ash, S. R. Worsfold, P. Vukusic, and G. R. Nash, en"A highly attenuating and frequency tailorable annular hole phononic crystal for surface acoustic waves," Nature Communications **8**, 174 (2017).

[39]M. Ghasemi Baboly, C. M. Reinke, B. A. Griffin, I. El-Kady, and Z. C. Leseman, en"Acoustic waveguiding in a silicon carbide phononic crystals at microwave frequencies," Applied Physics Letters **112**, 103504 (2018).

[40]Y. Wang, J. Lee, X.-Q. Zheng, Y. Xie, and P. X.-L. Feng, en"Hexagonal Boron Nitride Phononic Crystal Waveguides," ACS Photonics **6**, 3225–3232 (2019).

[41]S. Krödel and C. Daraio, en"Microlattice Metamaterials for Tailoring Ultrasonic Transmission with Elastoacoustic Hybridization," Physical Review Applied **6**, 064005 (2016).

[42]J.-C. Hsu and Y.-D. Lin, en"Microparticle concentration and separation inside a droplet using phononic-crystal scattered standing surface acoustic waves," Sensors and Actuators A: Physical **300**, 111651 (2019).

[43]X.-F. Li, X. Ni, L. Feng, M.-H. Lu, C. He, and Y.-F. Chen, en"Tunable Unidirectional Sound Propagation through a Sonic-Crystal-Based Acoustic Diode," Physical Review Letters **106**, 084301 (2011).

[44]E. Kim and J. Yang, "Review: Wave propagation in granular metamaterials," Functional Composites and Structures **1**, 012002 (2019).

[45]A. Vega-Flick, R. A. Duncan, S. P. Wallen, N. Boechler, C. Stelling, M. Retsch, J. J. Alvarado-Gil, K. A. Nelson, and A. A. Maznev, en"Vibrational dynamics of a two-dimensional microgranular crystal," Physical Review B **96**, 024303 (2017).

[46]A. Mehaney and A. M. Ahmed, en"Locally Resonant Phononic Crystals at Low frequencies Based on Porous SiC Multilayer," Scientific Reports **9**, 14767 (2019).

[47]S.-H. Jo, H. Yoon, Y. C. Shin, M. Kim, and B. D. Youn, en"Elastic wave localization and harvesting using double defect modes of a phononic crystal," Journal of Applied Physics **127**, 164901 (2020).

[48]A. Mehaney and A. A. S. Hassan, "Evolution of low-frequency phononic band gaps using quasi-periodic/defected phononic crystals," Materials Research Express **6**, 105801 (2019).

[49]F. Lucklum and M. Vellekoop, en"Design and Fabrication Challenges for Millimeter-Scale Three-Dimensional Phononic Crystals," Crystals **7**, 348 (2017).

[50]M. Vaezi, H. Seitz, and S. Yang, en"A review on 3D micro-additive manufacturing technologies," The International Journal of Advanced Manufacturing Technology **67**, 1721–1754 (2013).

[51]D. Beli, A. T. Fabro, M. Ruzzene, and J. R. F. Arruda, en"Wave attenuation and trapping in 3D printed cantilever-in-mass metamaterials with spatially correlated variability," Scientific Reports **9**, 5617 (2019).

[52]I.-C. Lee, N. Jeyaprakash, and C.-H. Yang, en"Characterization of ceramic phononic crystals prepared with additive manufacturing: Ultrasonic technique and finite element analysis," Ceramics International **46**, 27550–27560 (2020).

[53]Z. Tian and L. Yu, en"Rainbow trapping of ultrasonic guided waves in chirped phononic crystal plates," Scientific Reports **7**, 40004 (2017).

[54]K. L. Tsakmakidis, A. D. Boardman, and O. Hess, en"'Trapped rainbow' storage of light in metamaterials," Nature **450**, 397–401 (2007).

[55]Y. Y. Chen, R. Zhu, M. V. Barnhart, and G. L. Huang, en"Enhanced flexural wave sensing by adaptive gradient-index metamaterials," Scientific Reports **6**, 35048 (2016).

[56]H. Meng, D. Chronopoulos, A. Fabro, W. Elmadih, and I. Maskery, en"Rainbow metamaterials for broadband multi-frequency vibration attenuation: Numerical analysis and experimental validation," Journal of Sound and Vibration **465**, 115005 (2020).

[57]Z. Zhang, K. G. Demir, and G. X. Gu, en"Developments in 4D-printing: a review on current smart materials, technologies, and applications," International Journal of Smart and Nano Materials **10**, 205–224 (2019).

[58]X. K. Han and Z. Zhang, en"Topological Optimization of Phononic Crystal Thin Plate by a Genetic Algorithm," Scientific Reports **9**, 8331 (2019).

[59]S. Kumar and H. P. Lee, en"Recent Advances in Acoustic Metamaterials for Simultaneous Sound Attenuation and Air Ventilation Performances," Crystals **10**, 686 (2020).

[60]A. Bacigalupo, G. Gnecco, M. Lepidi, and L. Gambarotta, en"Machine-Learning Techniques for the Optimal Design of Acoustic Metamaterials," Journal of Optimization Theory and Applications **187**, 630–653 (2020).

[61]T. Brunet, J. Leng, and O. Mondain-Monval, en"Soft Acoustic Metamaterials," Science **342**, 323–324 (2013).

[62]J. Pierre, B. Dollet, and V. Leroy, en"Resonant Acoustic Propagation and Negative Density in Liquid Foams," Physical Review Letters **112**, 148307 (2014).

[63]B. Bonello, L. Belliard, J. Pierre, J. O. Vasseur, B. Perrin, and O. Boyko, en"Negative refraction of surface acoustic waves in the subgigahertz range," Physical Review B **82**, 104109 (2010).

[64]T. Brunet, A. Merlin, B. Mascaro, K. Zimny, J. Leng, O. Poncelet, C. Aristégui, and O. Mondain-Monval, en"Soft 3D acoustic metamaterial with negative index," Nature Materials **14**, 384–388 (2015).

[65]L. R. Meza, A. J. Zelhofer, N. Clarke, A. J. Mateos, D. M. Kochmann, and J. R. Greer, en"Resilient 3D hierarchical architected metamaterials," Proceedings of the National Academy of Sciences **112**, 11502–11507 (2015).

[66]D. Jang, L. R. Meza, F. Greer, and J. R. Greer, en"Fabrication and deformation of three-dimensional hollow ceramic nanostructures," Nature Materials **12**, 893–898 (2013).

[67]L. R. Meza, S. Das, and J. R. Greer, en"Strong, lightweight, and recoverable three-dimensional ceramic nanolattices," Science **345**, 1322–1326 (2014).

[68]R. H. Olsson III and I. El-Kady, "Microfabricated phononic crystal devices and applications," Measurement Science and Technology **20**, 012002 (2009).

[69]M. Eidini and G. H. Paulino, en"Unraveling metamaterial properties in zigzag-base folded sheets," Science Advances **1**, e1500224 (2015).

[70]J. T. Overvelde, T. A. de Jong, Y. Shevchenko, S. A. Becerra, G. M. Whitesides, J. C. Weaver, C. Hoberman, and K. Bertoldi, en"A three-dimensional actuated origami-inspired transformable metamaterial with multiple degrees of freedom," Nature Communications **7**, 10929 (2016).

[71]D. M. Sussman, Y. Cho, T. Castle, X. Gong, E. Jung, S. Yang, and R. D. Kamien, en"Algorithmic lattice kirigami: A route to pluripotent materials," Proceedings of the National Academy of Sciences **112**, 7449–7453 (2015).

[72]M. Kadic, T. Bückmann, N. Stenger, M. Thiel, and M. Wegener, en"On the practicability of pentamode mechanical metamaterials," Applied Physics Letters **100**, 191901 (2012).

[73]V. Romero Garcia and A.-C. Hladky-Hennion, English*Fundamentals and Applications of Acoustic Metamaterials: From Seismic to Radio Frequency* (ISTE, Ltd. ; John Wiley & Sons, Incorporated, London; Hoboken, NJ, 2019) oCLC: 1112423759.

[74]S. Benchabane, O. Gaiffe, R. Salut, G. Ulliac, V. Laude, and K. Kokkonen, en"Guidance of surface waves in a micron-scale phononic crystal line-defect waveguide," Applied Physics Letters **106**, 081903 (2015).

[75]D. Zhang, J. Zhao, B. Bonello, F. Zhang, W. Yuan, Y. Pan, and Z. Zhong, "Investigation of surface acoustic wave propagation in composite pillar based phononic crystals within both local resonance and Bragg scattering mechanism regimes," Journal of Physics D: Applied Physics **50**, 435602 (2017).

[76]D. B. Go, M. Z. Atashbar, Z. Ramshani, and H.-C. Chang, en"Surface acoustic wave devices for chemical sensing and microfluidics: a review and perspective," Analytical Methods **9**, 4112–4134 (2017).

[77]L. Y. Yeo and J. R. Friend, "Surface Acoustic Wave Microfluidics," Annual Review of Fluid Mechanics **46**, 379–406 (2014), publisher: Annual Reviews.

[78]R. J. Shilton, S. M. Langelier, J. R. Friend, and L. Y. Yeo, en"Surface acoustic wave solid-state rotational micromotor," Applied Physics Letters **100**, 033503 (2012).

[79]M. S. Faiz, M. Addouche, A. R. M. Zain, K. S. Siow, A. Chaalane, and A. Khelif, en"Experimental Demonstration of a Multichannel Elastic Wave Filter in a Phononic Crystal Slab," Applied Sciences **10**, 4594 (2020).

[80]M. Ghasemi Baboly, A. Raza, J. Brady, C. M. Reinke, Z. C. Leseman, and I. El-Kady, en"Demonstration of acoustic waveguiding and tight bending in phononic crystals," Applied Physics Letters **109**, 183504 (2016).

[81]G.-S. Liu, Y. Zhou, M.-H. Liu, Y. Yuan, X.-Y. Zou, and J.-C. Cheng, en"Acoustic waveguide with virtual soft boundary based on metamateri-

als," Scientific Reports **10**, 981 (2020).
[82]H. Pichard, A. Duclos, J.-P. Groby, V. Tournat, L. Zheng, and V. E. Gusev, en"Surface waves in granular phononic crystals," Physical Review E **93**, 023008 (2016).
[83]M. A. Porter, P. G. Kevrekidis, and C. Daraio, en"Granular crystals: Nonlinear dynamics meets materials engineering," Physics Today **68**, 44–50 (2015).
[84]G. Theocharis, N. Boechler, and C. Daraio, "Nonlinear Periodic Phononic Structures and Granular Crystals," in *Acoustic Metamaterials and Phononic Crystals*, Vol. 173, edited by P. A. Deymier (Springer Berlin Heidelberg, Berlin, Heidelberg, 2013) pp. 217–251, series Title: Springer Series in Solid-State Sciences.
[85]C. Chong, F. Li, J. Yang, M. O. Williams, I. G. Kevrekidis, P. G. Kevrekidis, and C. Daraio, en"Damped-driven granular chains: An ideal playground for dark breathers and multibreathers," Physical Review E **89**, 032924 (2014).
[86]A. Merkel, V. Tournat, and V. Gusev, en"Experimental Evidence of Rotational Elastic Waves in Granular Phononic Crystals," Physical Review Letters **107**, 225502 (2011).
[87]N. Boechler, G. Theocharis, and C. Daraio, en"Bifurcation-based acoustic switching and rectification," Nature Materials **10**, 665–668 (2011).
[88]F. Li, P. Anzel, J. Yang, P. G. Kevrekidis, and C. Daraio, en"Granular acoustic switches and logic elements," Nature Communications **5**, 5311 (2014).
[89]N. Boechler, J. K. Eliason, A. Kumar, A. A. Maznev, K. A. Nelson, and N. Fang, en"Interaction of a Contact Resonance of Microspheres with Surface Acoustic Waves," Physical Review Letters **111**, 036103 (2013).
[90]A. Khanolkar, S. Wallen, M. Abi Ghanem, J. Jenks, N. Vogel, and N. Boechler, en"A self-assembled metamaterial for Lamb waves," Applied Physics Letters **107**, 071903 (2015).
[91]J. K. Eliason, A. Vega-Flick, M. Hiraiwa, A. Khanolkar, T. Gan, N. Boechler, N. Fang, K. A. Nelson, and A. A. Maznev, en"Resonant attenuation of surface acoustic waves by a disordered monolayer of microspheres," Applied Physics Letters **108**, 061907 (2016).
[92]V. Babacic, J. Varghese, E. Coy, E. Kang, M. Pochylski, J. Gapinski, G. Fytas, and B. Graczykowski, en"Mechanical reinforcement of polymer colloidal crystals by supercritical fluids," Journal of Colloid and Interface Science **579**, 786–793 (2020).
[93]H. Kim, Y. Cang, E. Kang, B. Graczykowski, M. Secchi, M. Montagna, R. D. Priestley, E. M. Furst, and G. Fytas, en"Direct observation of polymer surface mobility via nanoparticle vibrations," Nature Communications **9**, 2918 (2018).
[94]M. Hiraiwa, M. Abi Ghanem, S. Wallen, A. Khanolkar, A. Maznev, and N. Boechler, en"Complex Contact-Based Dynamics of Microsphere Monolayers Revealed by Resonant Attenuation of Surface Acoustic Waves," Physical Review Letters **116**, 198001 (2016).
[95]L. Fan, H. Ge, S.-y. Zhang, H.-f. Gao, Y.-h. Liu, and H. Zhang, en"Nonlinear acoustic fields in acoustic metamaterial based on a cylindrical pipe with periodically arranged side holes," The Journal of the Acoustical Society of America **133**, 3846–3852 (2013).
[96]L. Fan, Z. Chen, Y.-c. Deng, J. Ding, H. Ge, S.-y. Zhang, Y.-t. Yang, and H. Zhang, en"Nonlinear effects in a metamaterial with double negativity," Applied Physics Letters **105**, 041904 (2014).
[97]Z. Chen, C. Xue, L. Fan, S.-y. Zhang, X.-j. Li, H. Zhang, and J. Ding, en"A tunable acoustic metamaterial with double-negativity driven by electromagnets," Scientific Reports **6**, 30254 (2016).
[98]K. J. B. Lee, M. K. Jung, and S. H. Lee, en"Highly tunable acoustic metamaterials based on a resonant tubular array," Physical Review B **86**, 184302 (2012).
[99]P. Wang, F. Casadei, S. Shan, J. C. Weaver, and K. Bertoldi, en"Harnessing Buckling to Design Tunable Locally Resonant Acoustic Metamaterials," Physical Review Letters **113**, 014301 (2014).
[100]J. J. Park, K. J. B. Lee, O. B. Wright, M. K. Jung, and S. H. Lee, en"Giant Acoustic Concentration by Extraordinary Transmission in Zero-Mass Metamaterials," Physical Review Letters **110**, 244302 (2013).
[101]Y. Jin, Y. Pennec, Y. Pan, and B. Djafari-Rouhani, en"Phononic Crystal Plate with Hollow Pillars Actively Controlled by Fluid Filling," Crystals **6**, 64 (2016).
[102]Z. Liang, M. Willatzen, J. Li, and J. Christensen, en"Tunable acoustic double negativity metamaterial," Scientific Reports **2**, 859 (2012).
[103]J. Wen, H. Shen, D. Yu, and X. Wen, en"Exploration of amphoteric and negative refraction imaging of acoustic sources via active metamaterials," Physics Letters A **377**, 2199–2206 (2013).
[104]B.-I. Popa, L. Zigoneanu, and S. A. Cummer, en"Tunable active acoustic metamaterials," Physical Review B **88**, 024303 (2013).
[105]S. Xiao, G. Ma, Y. Li, Z. Yang, and P. Sheng, en"Active control of membrane-type acoustic metamaterial by electric field," Applied Physics Letters **106**, 091904 (2015).
[106]G. Ma, X. Fan, P. Sheng, and M. Fink, en"Shaping reverberating sound fields with an actively tunable metasurface," Proceedings of the National Academy of Sciences **115**, 6638–6643 (2018).
[107]X. Chen, X. Xu, S. Ai, H. Chen, Y. Pei, and X. Zhou, en"Active acoustic metamaterials with tunable effective mass density by gradient magnetic fields," Applied Physics Letters **105**, 071913 (2014).
[108]S. Babaee, J. T. B. Overvelde, E. R. Chen, V. Tournat, and K. Bertoldi, en"Reconfigurable origami-inspired acoustic waveguides," Science Advances **2**, e1601019 (2016).
[109]T. Bückmann, M. Thiel, M. Kadic, R. Schittny, and M. Wegener, en"An elasto-mechanical unfeelability cloak made of pentamode metamaterials," Nature Communications **5**, 4130 (2014).
[110]P. Zhang and A. C. To, en"Broadband wave filtering of bioinspired hierarchical phononic crystal," Applied Physics Letters **102**, 121910 (2013).
[111]T. Chang, S. Jeon, M. Heo, and J. Shin, en"Mimicking bio-mechanical principles in photonic metamaterials for giant broadband nonlinearity," Communications Physics **3**, 79 (2020).
[112]S. Zhu, X. Tan, B. Wang, S. Chen, J. Hu, L. Ma, and L. Wu, en"Bio-inspired multistable metamaterials with reusable large deformation and ultra-high mechanical performance," Extreme Mechanics Letters **32**, 100548 (2019).
[113]W. Cheng, J. Wang, U. Jonas, G. Fytas, and N. Stefanou, en"Observation and tuning of hypersonic bandgaps in colloidal crystals," Nature Mater **5**, 830–836 (2006).
[114]G. Zhu, N. Z. Swinteck, S. Wu, J. S. Zhang, H. Pan, J. D. Bass, P. A. Deymier, D. Banerjee, and K. Yano, en"Direct observation of the phonon dispersion of a three-dimensional solid/solid hypersonic colloidal crystal," Phys. Rev. B **88**, 144307 (2013).
[115]A. S. Salasyuk, A. V. Scherbakov, D. R. Yakovlev, A. V. Akimov, A. A. Kaplyanskii, S. F. Kaplan, S. A. Grudinkin, A. V. Nashchekin, A. B. Pevtsov, V. G. Golubev, T. Berstermann, C. Brüggemann, M. Bombeck, and M. Bayer, en"Filtering of Elastic Waves by Opal-Based Hypersonic Crystal," Nano Lett. **10**, 1319–1323 (2010).
[116]P. J. Beltramo, D. Schneider, G. Fytas, and E. M. Furst, en"Anisotropic Hypersonic Phonon Propagation in Films of Aligned Ellipsoids," Phys. Rev. Lett. **113**, 205503 (2014).
[117]E. Alonso-Redondo, M. Schmitt, Z. Urbach, C. M. Hui, R. Sainidou, P. Rembert, K. Matyjaszewski, M. R. Bockstaller, and G. Fytas, en"A new class of tunable hypersonic phononic crystals based on polymer-tethered colloids," Nat Commun **6**, 8309 (2015).
[118]B. Graczykowski, N. Vogel, K. Bley, H.-J. Butt, and G. Fytas, en"Multiband Hypersound Filtering in Two-Dimensional Colloidal Crystals: Adhesion, Resonances, and Periodicity," Nano Lett. **20**, 1883–1889 (2020).
[119]B. Graczykowski, M. Sledzinska, F. Alzina, J. Gomis-Bresco, J. S. Reparaz, M. R. Wagner, and C. M. Sotomayor Torres, en"Phonon dispersion in hypersonic two-dimensional phononic crystal membranes," Phys. Rev. B **91**, 075414 (2015).
[120]R. Dehghannasiri, A. A. Eftekhar, and A. Adibi, en"Hypersonic Surface Phononic Bandgap Demonstration in a CMOS-Compatible Pillar-Based Piezoelectric Structure on Silicon," Phys. Rev. Applied **10**, 064019 (2018).
[121]M. R. Wagner, B. Graczykowski, J. S. Reparaz, A. El Sachat, M. Sledzinska, F. Alzina, and C. M. Sotomayor Torres, en"Two-Dimensional Phononic Crystals: Disorder Matters," Nano Lett. **16**, 5661–5668 (2016).
[122]G. N. Aliev and B. Goller, en"Quasi-periodic Fibonacci and periodic one-dimensional hypersonic phononic crystals of porous silicon: Experiment and simulation," Journal of Applied Physics **116**, 094903 (2014).
[123]B. Graczykowski, M. Sledzinska, N. Kehagias, F. Alzina, J. S. Reparaz, and C. M. Sotomayor Torres, en"Hypersonic phonon propagation in one-dimensional surface phononic crystal," Appl. Phys. Lett. **104**, 123108 (2014).
[124]S. Wu, G. Zhu, J. S. Zhang, D. Banerjee, J. D. Bass, C. Ling, and K. Yano,

en“Anisotropic lattice expansion of three-dimensional colloidal crystals and its impact on hypersonic phonon band gaps,” Phys. Chem. Chem. Phys. **16**, 8921 (2014).

[125]M. Sledzinska, B. Graczykowski, F. Alzina, J. Santiso Lopez, and C. Sotomayor Torres, en“Fabrication of phononic crystals on free-standing silicon membranes,” Microelectronic Engineering **149**, 41–45 (2016).

[126]D. Nardi, M. Travagliati, M. E. Siemens, Q. Li, M. M. Murnane, H. C. Kapteyn, G. Ferrini, F. Parmigiani, and F. Banfi, en“Probing Thermomechanics at the Nanoscale: Impulsively Excited Pseudosurface Acoustic Waves in Hypersonic Phononic Crystals,” Nano Lett. **11**, 4126–4133 (2011).

[127]M. Travagliati, D. Nardi, C. Giannetti, V. Gusev, P. Pingue, V. Piazza, G. Ferrini, and F. Banfi, en“Interface nano-confined acoustic waves in polymeric surface phononic crystals,” Appl. Phys. Lett. **106**, 021906 (2015).

[128]T.-W. Liu, Y.-C. Tsai, Y.-C. Lin, T. Ono, S. Tanaka, and T.-T. Wu, en“Design and fabrication of a phononic-crystal-based Love wave resonator in GHz range,” AIP Advances **4**, 124201 (2014).

[129]D. Yudistira, A. Boes, B. Graczykowski, F. Alzina, L. Y. Yeo, C. M. Sotomayor Torres, and A. Mitchell, en“Nanoscale pillar hypersonic surface phononic crystals,” Phys. Rev. B **94**, 094304 (2016).

[130]A. M. Rakhymzhanov, A. Gueddida, E. Alonso-Redondo, Z. N. Utegulov, D. Perevoznik, K. Kurselis, B. N. Chichkov, E. H. El Boudouti, B. Djafari-Rouhani, and G. Fytas, en“Band structure of cavity-type hypersonic phononic crystals fabricated by femtosecond laser-induced two-photon polymerization,” Appl. Phys. Lett. **108**, 201901 (2016).

[131]M. Ghasemi Baboly, S. Alaie, C. M. Reinke, I. El-Kady, and Z. C. Leseman, en“Ultra-high frequency, high Q/volume micromechanical resonators in a planar AlN phononic crystal,” Journal of Applied Physics **120**, 034502 (2016).

[132]R. Pourabolghasem, R. Dehghannasiri, A. A. Eftekhar, and A. Adibi, en“Waveguiding Effect in the Gigahertz Frequency Range in Pillar-based Phononic-Crystal Slabs,” Phys. Rev. Applied **9**, 014013 (2018).

[133]C. Y. T. Huang, F. Kargar, T. Debnath, B. Debnath, M. D. Valentin, R. Synowicki, S. Schoeche, R. K. Lake, and A. A. Balandin, “Phononic and photonic properties of shape-engineered silicon nanoscale pillar arrays,” Nanotechnology **31**, 30LT01 (2020).

[134]V. L. Zhang, C. G. Hou, H. H. Pan, F. S. Ma, M. H. Kuok, H. S. Lim, S. C. Ng, M. G. Cottam, M. Jamali, and H. Yang, en“Phononic dispersion of a two-dimensional chessboard-patterned bicomponent array on a substrate,” Appl. Phys. Lett. **101**, 053102 (2012).

[135]R. Sainidou, N. Stefanou, and A. Modinos, en“Widening of Phononic Transmission Gaps via Anderson Localization,” Phys. Rev. Lett. **94**, 205503 (2005).

[136]G. Gkantzounis, T. Amoah, and M. Florescu, en“Hyperuniform disordered phononic structures,” Phys. Rev. B **95**, 094120 (2017).

[137]N. Yazdani, M. Jansen, D. Bozyigit, W. M. M. Lin, S. Volk, O. Yarema, M. Yarema, F. Juranyi, S. D. Huber, and V. Wood, “Nanocrystal superlattices as phonon-engineered solids and acoustic metamaterials,” **10**, 4236, number: 1 Publisher: Nature Publishing Group.

[138]B. Munkhbat, A. B. Yankovich, D. G. Baranov, R. Verre, E. Olsson, and T. O. Shegai, en“Transition metal dichalcogenide metamaterials with atomic precision,” Nat Commun **11**, 4604 (2020).

[139]K. S. Novoselov, A. Mishchenko, A. Carvalho, and A. H. C. Neto, “2d materials and van der waals heterostructures,” **353**, aac9439, number: 6298 Reporter: Science.

[140]L. C. Parsons and G. T. Andrews, en“Brillouin scattering from porous silicon-based optical Bragg mirrors,” Journal of Applied Physics **111**, 123521 (2012).

[141]N. D. Lanzillotti-Kimura, A. Fainstein, A. Lemaitre, B. Jusserand, and B. Perrin, en“Coherent control of sub-terahertz confined acoustic nanowaves: Theory and experiments,” Phys. Rev. B **84**, 115453 (2011).

[142]P. M. Walker, J. S. Sharp, A. V. Akimov, and A. J. Kent, en“Coherent elastic waves in a one-dimensional polymer hypersonic crystal,” Appl. Phys. Lett. **97**, 073106 (2010).

[143]F. Döring, H. Ulrichs, S. Pagel, M. Müller, M. Mansurova, M. Müller, C. Eberl, T. Erichsen, D. Huebner, P. Vana, K. Mann, M. Münzenberg, and H.-U. Krebs, “Confinement of phonon propagation in laser deposited tungsten/polycarbonate multilayers,” New J. Phys. **18**, 092002 (2016).

[144]D. Schneider, F. Liaqat, E. H. El Boudouti, O. El Abouti, W. Tremel, H.-J. Butt, B. Djafari-Rouhani, and G. Fytas, en“Defect-Controlled Hypersound Propagation in Hybrid Superlattices,” Phys. Rev. Lett. **111**, 164301 (2013).

[145]N. Gomopoulos, D. Maschke, C. Y. Koh, E. L. Thomas, W. Tremel, H.-J. Butt, and G. Fytas, en“One-Dimensional Hypersonic Phononic Crystals,” Nano Lett. **10**, 980–984 (2010).

[146]Z. Lazcano, O. Meza, and J. Arriaga, en“Localization of acoustic modes in periodic porous silicon structures,” Nanoscale Res Lett **9**, 419 (2014).

[147]G. Arregui, N. Lanzillotti-Kimura, C. Sotomayor-Torres, and P. García, en“Anderson Photon-Phonon Colocalization in Certain Random Superlattices,” Phys. Rev. Lett. **122**, 043903 (2019).

[148]G. Wu, Y. Zhu, S. Merugu, N. Wang, C. Sun, and Y. Gu, “Ghz spurious mode free aln lamb wave resonator with high figure of merit using one dimensional phononic crystal tethers,” Applied Physics Letters **109**, 013506 (2016), https://doi.org/10.1063/1.4955410.

[149]H. Fu, en“Colloidal metal halide perovskite nanocrystals: a promising juggernaut in photovoltaic applications,” J. Mater. Chem. A **7**, 14357–14379 (2019).

[150]J. Chang and E. R. Waclawik, en“Colloidal semiconductor nanocrystals: controlled synthesis and surface chemistry in organic media,” RSC Adv. **4**, 23505–23527 (2014).

[151]Dmitri V. Talapin, Elena V. Shevchenko, Andreas Kornowski, Nikolai Gaponik, Markus Haase, Andrey L. Rogach, and Horst Weller, “A New Approach to Crystallization of CdSe Nanoparticles into Ordered Three-Dimensional Superlattices,” Advanced Materials **13**, 1868–1871 (2001).

[152]X.-H. Li, J.-X. Li, G.-D. Li, D.-P. Liu, and J.-S. Chen, en“Controlled Synthesis, Growth Mechanism, and Properties of Monodisperse CdS Colloidal Spheres,” Chem. Eur. J. **13**, 8754–8761 (2007).

[153]Margaret A. Hines and Gregory D. Scholes, “Colloidal PbS Nanocrystals with Size-Tunable Near-Infrared Emission: Observation of Post-Synthesis Self-Narrowing of the Particle Size Distribution,” Advanced Materials **15**, 1844–1849 (2003).

[154]C. L. Poyser, T. Czerniuk, A. Akimov, B. T. Diroll, E. A. Gaulding, A. S. Salasyuk, A. J. Kent, D. R. Yakovlev, M. Bayer, and C. B. Murray, en“Coherent Acoustic Phonons in Colloidal Semiconductor Nanocrystal Superlattices,” ACS Nano **10**, 1163–1169 (2016).

[155]A. Mondal, J. Aneesh, V. Kumar Ravi, R. Sharma, W. J. Mir, M. C. Beard, A. Nag, and K. V. Adarsh, en“Ultrafast exciton many-body interactions and hot-phonon bottleneck in colloidal cesium lead halide perovskite nanocrystals,” Phys. Rev. B **98**, 115418 (2018).

[156]K. Chen, S. Schünemann, and H. Tüysüz, en“Preparation of Waterproof Organometal Halide Perovskite Photonic Crystal Beads,” Angew. Chem. **129**, 6648–6652 (2017).

[157]K. E. Knowles, K. H. Hartstein, T. B. Kilburn, A. Marchioro, H. D. Nelson, P. J. Whitham, and D. R. Gamelin, en“Luminescent Colloidal Semiconductor Nanocrystals Containing Copper: Synthesis, Photophysics, and Applications,” Chem. Rev. **116**, 10820–10851 (2016).

[158]S. Schünemann, S. Brittman, K. Chen, E. C. Garnett, and H. Tüysüz, en“Halide Perovskite 3D Photonic Crystals for Distributed Feedback Lasers,” ACS Photonics **4**, 2522–2528 (2017).

[159]H. Seiler, S. Palato, C. Sonnichsen, H. Baker, E. Socie, D. P. Strandell, and P. Kambhampati, “Two-dimensional electronic spectroscopy reveals liquid-like lineshape dynamics in CsPbI3 perovskite nanocrystals,” Nature Communications **10**, 4962 (2019).

[160]H. Seiler, S. Palato, and P. Kambhampati, “Investigating exciton structure and dynamics in colloidal cdse quantum dots with two-dimensional electronic spectroscopy,” The Journal of Chemical Physics **149**, 074702 (2018), https://doi.org/10.1063/1.5037223.

[161]M. Khosla, S. Rao, and S. Gupta, “Polarons Explain Luminescence Behavior of Colloidal Quantum Dots at Low Temperature,” Scientific Reports **8**, 8385 (2018).

[162]P.-A. Mante, C. C. Stoumpos, M. G. Kanatzidis, and A. Yartsev, “Electron–acoustic phonon coupling in single crystal CH3NH3PbI3 perovskites revealed by coherent acoustic phonons,” Nature Communications **8**, 14398 (2017).

[163]D. Oron, A. Aharoni, C. de Mello Donega, J. van Rijssel, A. Meijerink, and U. Banin, “Universal role of discrete acoustic phonons in the low-temperature optical emission of colloidal quantum dots,” Phys. Rev. Lett. **102**, 177402 (2009).

[164]B. Villa, A. J. Bennett, D. J. P. Ellis, J. P. Lee, J. Skiba-Szymanska, T. A.

Mitchell, J. P. Griffiths, I. Farrer, D. A. Ritchie, C. J. B. Ford, and A. J. Shields, "Surface acoustic wave modulation of a coherently driven quantum dot in a pillar microcavity," Applied Physics Letters **111**, 011103 (2017), https://doi.org/10.1063/1.4990966.

[165] P. Delsing, A. N. Cleland, M. J. A. Schuetz, J. Knörzer, G. Giedke, J. I. Cirac, K. Srinivasan, M. Wu, K. C. Balram, C. Bäuerle, T. Meunier, C. J. B. Ford, P. V. Santos, E. Cerda-Méndez, H. Wang, H. J. Krenner, E. D. S. Nysten, M. Weiß, G. R. Nash, L. Thevenard, C. Gourdon, P. Rovillain, M. Marangolo, J.-Y. Duquesne, G. Fischerauer, W. Ruile, A. Reiner, B. Paschke, D. Denysenko, D. Volkmer, A. Wixforth, H. Bruus, M. Wiklund, J. Reboud, J. M. Cooper, Y. Fu, M. S. Brugger, F. Rehfeldt, and C. Westerhausen, "The 2019 surface acoustic waves roadmap," Journal of Physics D: Applied Physics **52**, 353001 (2019).

[166] J. Pei, J. Yang, X. Wang, F. Wang, S. Mokkapati, T. Lü, J.-C. Zheng, Q. Qin, D. Neshev, H. H. Tan, C. Jagadish, and Y. Lu, en"Excited State Biexcitons in Atomically Thin MoSe $_2$," ACS Nano **11**, 7468–7475 (2017).

[167] Y. Yang, X. Li, M. Wen, E. Hacopian, W. Chen, Y. Gong, J. Zhang, B. Li, W. Zhou, P. M. Ajayan, Q. Chen, T. Zhu, and J. Lou, en"Brittle Fracture of 2D MoSe $_2$," Adv. Mater. **29**, 1604201 (2017).

[168] M. Sledzinska, B. Graczykowski, M. Placidi, D. S. Reig, A. E. Sachat, J. S. Reparaz, F. Alzina, B. Mortazavi, R. Quey, L. Colombo, S. Roche, and C. M. S. Torres, "Thermal conductivity of MoS $_2$ polycrystalline nanomembranes," 2D Mater. **3**, 035016 (2016).

[169] S. Bertolazzi, J. Brivio, and A. Kis, en"Stretching and Breaking of Ultrathin MoS $_2$," ACS Nano **5**, 9703–9709 (2011).

[170] X. Zhang, C. De-Eknamkul, J. Gu, A. L. Boehmke, V. M. Menon, J. Khurgin, and E. Cubukcu, en"Guiding of visible photons at the ångström thickness limit," Nat. Nanotechnol. **14**, 844–850 (2019).

[171] V. Nicolosi, M. Chhowalla, M. G. Kanatzidis, M. S. Strano, and J. N. Coleman, en"Liquid Exfoliation of Layered Materials," Science **340**, 1226419–1226419 (2013).

[172] H. Li, J. Wu, Z. Yin, and H. Zhang, en"Preparation and Applications of Mechanically Exfoliated Single-Layer and Multilayer MoS $_2$ and WSe $_2$ Nanosheets," Acc. Chem. Res. **47**, 1067–1075 (2014).

[173] T. Yun, H. M. Jin, D. Kim, K. H. Han, G. G. Yang, G. Y. Lee, G. S. Lee, J. Y. Choi, I. Kim, and S. O. Kim, en"2D Metal Chalcogenide Nanopatterns by Block Copolymer Lithography," Adv. Funct. Mater. **28**, 1804508 (2018).

[174] J. P. Thiruraman, P. Masih Das, and M. Drndić, en"Irradiation of Transition Metal Dichalcogenides Using a Focused Ion Beam: Controlled Single-Atom Defect Creation," Adv. Funct. Mater. **29**, 1904668 (2019).

[175] R. Kozubek, M. Tripathi, M. Ghorbani-Asl, S. Kretschmer, L. Madauß, E. Pollmann, M. O'Brien, N. McEvoy, U. Ludacka, T. Susi, G. S. Duesberg, R. A. Wilhelm, A. V. Krasheninnikov, J. Kotakoski, and M. Schleberger, en"Perforating Freestanding Molybdenum Disulfide Monolayers with Highly Charged Ions," J. Phys. Chem. Lett. **10**, 904–910 (2019).

[176] D. S. Fox, Y. Zhou, P. Maguire, A. O'Neill, C. Ó'Coileáin, R. Gatensby, A. M. Glushenkov, T. Tao, G. S. Duesberg, I. V. Shvets, M. Abid, M. Abid, H.-C. Wu, Y. Chen, J. N. Coleman, J. F. Donegan, and H. Zhang, en"Nanopatterning and Electrical Tuning of MoS $_2$ Layers with a Subnanometer Helium Ion Beam," Nano Lett. **15**, 5307–5313 (2015).

[177] T. Vasileiadis, H. Zhang, H. Wang, M. Bonn, G. Fytas, and B. Graczykowski, "Frequency-domain study of nonthermal gigahertz phonons reveals fano coupling to charge carriers," Science Advances **6** (2020), 10.1126/sciadv.abd4540, https://advances.sciencemag.org/content/6/51/eabd4540.full.pdf.

[178] M. Eichenfield, J. Chan, R. M. Camacho, K. J. Vahala, and O. Painter, "Optomechanical crystals," Nature **462**, 78–82 (2009).

[179] J. Chan, T. M. Alegre, A. H. Safavi-Naeini, J. T. Hill, A. Krause, S. Gröblacher, M. Aspelmeyer, and O. Painter, "Laser cooling of a nanomechanical oscillator into its quantum ground state," Nature **478**, 89–92 (2011).

[180] K. Fang, M. H. Matheny, X. Luan, and O. Painter, "Optical transduction and routing of microwave phonons in cavity-optomechanical circuits," Nature Photonics **10**, 489–496 (2016).

[181] D. Navarro-Urrios, N. E. Capuj, J. Gomis-Bresco, F. Alzina, A. Pitanti, A. Griol, A. Martínez, and C. S. Torres, "A self-stabilized coherent phonon source driven by optical forces," Scientific reports **5**, 1–7 (2015).

[182] M. Bagheri, M. Poot, M. Li, W. P. Pernice, and H. X. Tang, "Dynamic manipulation of nanomechanical resonators in the high-amplitude regime and non-volatile mechanical memory operation," Nature nanotechnology **6**, 726–732 (2011).

[183] A. G. Krause, M. Winger, T. D. Blasius, Q. Lin, and O. Painter, "A high-resolution microchip optomechanical accelerometer," Nature Photonics **6**, 768 (2012).

[184] A. H. Safavi-Naeini, T. M. Alegre, J. Chan, M. Eichenfield, M. Winger, Q. Lin, J. T. Hill, D. E. Chang, and O. Painter, "Electromagnetically induced transparency and slow light with optomechanics," Nature **472**, 69–73 (2011).

[185] V. Peano, C. Brendel, M. Schmidt, and F. Marquardt, "Topological phases of sound and light," Physical Review X **5**, 031011 (2015).

[186] J. Gomis-Bresco, D. Navarro-Urrios, M. Oudich, S. El-Jallal, A. Griol, D. Puerto, E. Chavez, Y. Pennec, B. Djafari-Rouhani, F. Alzina, *et al.*, "A one-dimensional optomechanical crystal with a complete phononic band gap," Nature communications **5**, 1–6 (2014).

[187] A. H. Safavi-Naeini, J. T. Hill, S. Meenehan, J. Chan, S. Gröblacher, and O. Painter, "Two-dimensional phononic-photonic band gap optomechanical crystal cavity," Physical Review Letters **112**, 153603 (2014).

[188] G. Heinrich, M. Ludwig, J. Qian, B. Kubala, and F. Marquardt, "Collective dynamics in optomechanical arrays," Physical review letters **107**, 043603 (2011).

[189] K. Pelka, V. Peano, and A. Xuereb, "Chimera states in small optomechanical arrays," Physical Review Research **2**, 013201 (2020).

[190] M. F. Colombano, G. Arregui, N. E. Capuj, A. Pitanti, J. Maire, A. Griol, B. Garrido, A. Martínez, C. M. Sotomayor-Torres, and D. Navarro-Urrios, "Synchronization of optomechanical nanobeams by mechanical interaction," Physical review letters **123**, 017402 (2019).

[191] M. Zhang, S. Shah, J. Cardenas, and M. Lipson, "Synchronization and phase noise reduction in micromechanical oscillator arrays coupled through light," Physical review letters **115**, 163902 (2015).

[192] J. T. Hill, A. H. Safavi-Naeini, J. Chan, and O. Painter, "Coherent optical wavelength conversion via cavity optomechanics," Nature communications **3**, 1–7 (2012).

[193] R. Singh and T. P. Purdy, "Detecting acoustic blackbody radiation with an optomechanical antenna," Physical Review Letters **125**, 120603 (2020).

[194] W. Jiang, C. J. Sarabalis, Y. D. Dahmani, R. N. Patel, F. M. Mayor, T. P. McKenna, R. Van Laer, and A. H. Safavi-Naeini, "Efficient bidirectional piezo-optomechanical transduction between microwave and optical frequency," Nature communications **11**, 1–7 (2020).

[195] G. S. MacCabe, H. Ren, J. Luo, J. D. Cohen, H. Zhou, A. Sipahigil, M. Mirhosseini, and O. Painter, "Nano-acoustic resonator with ultralong phonon lifetime," Science **370**, 840–843 (2020).

[196] A. H. Ghadimi, S. A. Fedorov, N. J. Engelsen, M. J. Bereyhi, R. Schilling, D. J. Wilson, and T. J. Kippenberg, "Elastic strain engineering for ultralow mechanical dissipation," Science **360**, 764–768 (2018).

[197] H. Ren, T. Shah, H. Pfeifer, C. Brendel, V. Peano, F. Marquardt, and O. Painter, "Topological phonon transport in an optomechanical system," arXiv preprint arXiv:2009.06174 (2020).

[198] P. YU and M. Cardona, *Fundamentals of Semiconductors: Physics and Materials Properties*, 4th ed., Graduate Texts in Physics (Springer-Verlag) version Number: 4.

[199] D. G. Cahill, W. K. Ford, K. E. Goodson, G. D. Mahan, A. Majumdar, H. J. Maris, R. Merlin, and S. R. Phillpot, "Nanoscale thermal transport," **93**, 793–818 (), number: 2 Reporter: Journal of Applied Physics.

[200] G. Chen, *Nanoscale Energy Transport and Conversion: A Parallel Treatment of Electrons, Molecules, Phonons, and Photons* (Oxford University Press) google-Books-ID: M3n3lUJpYDYC.

[201] D. G. Cahill, P. V. Braun, G. Chen, D. R. Clarke, S. Fan, K. E. Goodson, P. Keblinski, W. P. King, G. D. Mahan, A. Majumdar, H. J. Maris, S. R. Phillpot, E. Pop, and L. Shi, "Nanoscale thermal transport. II. 2003–2012," **1**, 011305 (), number: 1 Reporter: Applied Physics Reviews.

[202] S. Volz, J. Ordonez-Miranda, A. Shchepetov, M. Prunnila, J. Ahopelto, T. Pezeril, G. Vaudel, V. Gusev, P. Ruello, E. M. Weig, M. Schubert, M. Hettich, M. Grossman, T. Dekorsy, F. Alzina, B. Graczykowski, E. Chavez-Angel, J. Sebastian Reparaz, M. R. Wagner, C. M. Sotomayor-Torres, S. Xiong, S. Neogi, and D. Donadio, "Nanophononics: state of the art and perspectives," **89**, 15, number: 1 Reporter: The European Physical Journal B.

[203] J. Lee, W. Lee, G. Wehmeyer, S. Dhuey, D. L. Olynick, S. Cabrini, C. Dames, J. J. Urban, and P. Yang, "Investigation of phonon coherence

and backscattering using silicon nanomeshes," **8**, 14054, reporter: Nature Communications.
[204]J.-K. Yu, S. Mitrovic, D. Tham, J. Varghese, and J. R. Heath, "Reduction of thermal conductivity in phononic nanomesh structures," **5**, 718–721, number: 10 Reporter: Nature Nanotechnology.
[205]B. Graczykowski, A. E. Sachat, J. S. Reparaz, M. Sledzinska, M. R. Wagner, E. Chavez-Angel, Y. Wu, S. Volz, Y. Wu, F. Alzina, and C. M. S. Torres, "Thermal conductivity and air-mediated losses in periodic porous silicon membranes at high temperatures," **8**, 415, number: 1 Reporter: Nature Communications.
[206]M. Sledzinska, B. Graczykowski, F. Alzina, U. Melia, K. Termentzidis, D. Lacroix, and C. M. S. Torres, "Thermal conductivity in disordered porous nanomembranes," (), 10.1088/1361-6528/ab0ecd, reporter: Nanotechnology.
[207]M. Nomura, J. Nakagawa, Y. Kage, J. Maire, D. Moser, and O. Paul, "Thermal phonon transport in silicon nanowires and two-dimensional phononic crystal nanostructures," **106**, 143102, number: 14 Reporter: Applied Physics Letters.
[208]J. Maire, R. Anufriev, R. Yanagisawa, A. Ramiere, S. Volz, and M. Nomura, "Heat conduction tuning by wave nature of phonons," **3**, e1700027, number: 8 Reporter: Science Advances.
[209]N. Zen, T. A. Puurtinen, T. J. Isotalo, S. Chaudhuri, and I. J. Maasilta, "Engineering thermal conductance using a two-dimensional phononic crystal," **5**, 3435, reporter: Nature Communications.
[210]J. Lim, H.-T. Wang, J. Tang, S. C. Andrews, H. So, J. Lee, D. H. Lee, T. P. Russell, and P. Yang, "Simultaneous thermoelectric property measurement and incoherent phonon transport in holey silicon," **10**, 124–132, number: 1 Reporter: ACS Nano.
[211]J. Tang, H.-T. Wang, D. H. Lee, M. Fardy, Z. Huo, T. P. Russell, and P. Yang, "Holey silicon as an efficient thermoelectric material," **10**, 4279–4283, number: 10 Reporter: Nano Letters.
[212]M. N. Luckyanova, J. Garg, K. Esfarjani, A. Jandl, M. T. Bulsara, A. J. Schmidt, A. J. Minnich, S. Chen, M. S. Dresselhaus, Z. Ren, E. A. Fitzgerald, and G. Chen, "Coherent phonon heat conduction in superlattices," **338**, 936–939 (), publisher: American Association for the Advancement of Science Section: Report.
[213]M. N. Luckyanova, J. Mendoza, H. Lu, B. Song, S. Huang, J. Zhou, M. Li, Y. Dong, H. Zhou, J. Garlow, L. Wu, B. J. Kirby, A. J. Grutter, A. A. Puretzky, Y. Zhu, M. S. Dresselhaus, A. Gossard, and G. Chen, "Phonon localization in heat conduction," **4**, eaat9460 (), publisher: American Association for the Advancement of Science Section: Research Article.
[214]J. Ravichandran, A. K. Yadav, R. Cheaito, P. B. Rossen, A. Soukiassian, S. J. Suresha, J. C. Duda, B. M. Foley, C.-H. Lee, Y. Zhu, A. W. Lichtenberger, J. E. Moore, D. A. Muller, D. G. Schlom, P. E. Hopkins, A. Majumdar, R. Ramesh, and M. A. Zurbuchen, "Crossover from incoherent to coherent phonon scattering in epitaxial oxide superlattices," **13**, 168–172, number: 2 Publisher: Nature Publishing Group.
[215]K. Takahashi, M. Fujikane, Y. Liao, M. Kashiwagi, T. Kawasaki, N. Tambo, S. Ju, Y. Naito, and J. Shiomi, "Elastic inhomogeneity and anomalous thermal transport in ultrafine si phononic crystals," **71**, 104581.
[216]M. Kasprzak, M. Sledzinska, K. Zaleski, I. Iatsunskyi, F. Alzina, S. Volz, C. M. Sotomayor Torres, and B. Graczykowski, "High-temperature silicon thermal diode and switch," **78**, 105261.
[217]N. Tambo, Y. Liao, C. Zhou, E. M. Ashley, K. Takahashi, P. F. Nealey, Y. Naito, and J. Shiomi, "Ultimate suppression of thermal transport in amorphous silicon nitride by phononic nanostructure," **6**, eabc0075, publisher: American Association for the Advancement of Science Section: Research Article.
[218]S. Alaie, D. F. Goettler, M. Su, Z. C. Leseman, C. M. Reinke, and I. El-Kady, "Thermal transport in phononic crystals and the observation of coherent phonon scattering at room temperature," **6**, 7228, reporter: Nature Communications.
[219]P. E. Hopkins, C. M. Reinke, M. F. Su, R. H. Olsson, E. A. Shaner, Z. C. Leseman, J. R. Serrano, L. M. Phinney, and I. El-Kady, "Reduction in the thermal conductivity of single crystalline silicon by phononic crystal patterning," **11**, 107–112, number: 1 Reporter: Nano Letters.
[220]M. Sledzinska, B. Graczykowski, J. Maire, E. Chavez-Angel, C. M. Sotomayor-Torres, and F. Alzina, "2d phononic crystals: Progress and prospects in hypersound and thermal transport engineering," **30**, 1904434 (), _eprint: https://onlinelibrary.wiley.com/doi/pdf/10.1002/adfm.201904434.
[221]G. Xie, D. Ding, and G. Zhang, "Phonon coherence and its effect on thermal conductivity of nanostructures," **3**, 1480417, publisher: Taylor & Francis _eprint: https://doi.org/10.1080/23746149.2018.1480417.
[222]R. Anufriev, A. Ramiere, J. Maire, and M. Nomura, "Heat guiding and focusing using ballistic phonon transport in phononic nanostructures," **8**, 15505, number: 1 Publisher: Nature Publishing Group.
[223]X. Huang, D. Ohori, R. Yanagisawa, R. Anufriev, S. Samukawa, and M. Nomura, "Coherent and incoherent impacts of nanopillars on the thermal conductivity in silicon nanomembranes," **12**, 25478–25483 (), publisher: American Chemical Society.
[224]W. Chen, D. Talreja, D. Eichfeld, P. Mahale, N. N. Nova, H. Y. Cheng, J. L. Russell, S.-Y. Yu, N. Poilvert, G. Mahan, S. E. Mohney, V. H. Crespi, T. E. Mallouk, J. V. Badding, B. Foley, V. Gopalan, and I. Dabo, "Achieving minimal heat conductivity by ballistic confinement in phononic metalattices," **14**, 4235–4243, publisher: American Chemical Society.
[225]Q. Hao, D. Xu, H. Zhao, Y. Xiao, and F. J. Medina, "Thermal studies of nanoporous si films with pitches on the order of 100 nm —comparison between different pore-drilling techniques," **8**, 9056, number: 1 Publisher: Nature Publishing Group.
[226]A. Jain, Y.-J. Yu, and A. J. H. McGaughey, "Phonon transport in periodic silicon nanoporous films with feature sizes greater than 100 nm," **87**, 195301, publisher: American Physical Society.
[227]N. Jaziri, A. Boughamoura, J. Müller, B. Mezghani, F. Tounsi, and M. Ismail, "A comprehensive review of thermoelectric generators: Technologies and common applications," 10.1016/j.egyr.2019.12.011.
[228]D. S. Trimmer, *CRC Handbook of Thermoelectrics* (CRC Press).
[229]J.-P. Colinge, *Silicon-on-Insulator Technology: Materials to VLSI*, 2nd ed. (Springer US).
[230]A. Sharif, *Harsh Environment Electronics: Interconnect Materials and Performance Assessment* (John Wiley & Sons) google-Books-ID: FF2NDwAAQBAJ.
[231]B. L. Davis and M. I. Hussein, "Nanophononic metamaterial: Thermal conductivity reduction by local resonance," **112**, 055505, number: 5 Reporter: Physical Review Letters.
[232]M. I. Hussein, C.-N. Tsai, and H. Honarvar, "Thermal conductivity reduction in a nanophononic metamaterial versus a nanophononic crystal: A review and comparative analysis," **30**, 1906718, _eprint: https://onlinelibrary.wiley.com/doi/pdf/10.1002/adfm.201906718.
[233]X. Huang, S. Gluchko, R. Anufriev, S. Volz, and M. Nomura, "Thermal conductivity reduction in a silicon thin film with nanocones," **11**, 34394–34398 (), publisher: American Chemical Society.
[234]Y. Wu, J. Ordonez-Miranda, S. Gluchko, R. Anufriev, D. D. S. Meneses, L. D. Campo, S. Volz, and M. Nomura, "Enhanced thermal conduction by surface phonon-polaritons," **6**, eabb4461, publisher: American Association for the Advancement of Science Section: Research Article.
[235]G. E. W. Bauer, E. Saitoh, and B. J. van Wees, "Spin caloritronics," **11**, 391–399, number: 5 Publisher: Nature Publishing Group.
[236]S. R. Boona, R. C. Myers, and J. P. Heremans, "Spin caloritronics," **7**, 885–910, publisher: The Royal Society of Chemistry.
[237]J. Cunha, T.-L. Guo, G. D. Valle, A. N. Koya, R. P. Zaccaria, and A. Alabastri, "Controlling light, heat, and vibrations in plasmonics and phononics," **n/a**, 2001225, _eprint: https://onlinelibrary.wiley.com/doi/pdf/10.1002/adom.202001225.
[238]F. A. Nutz and M. Retsch, "Tailor-made temperature-dependent thermal conductivity via interparticle constriction," **3**, eaao5238, number: 11 Reporter: Science Advances.
[239]F. A. Nutz, A. Philipp, B. A. F. Kopera, M. Dulle, and M. Retsch, "Low thermal conductivity through dense particle packings with optimum disorder," 10.1002/adma.201704910, reporter: Advanced Materials.
[240]B. Li, L. Wang, and G. Casati, "Thermal diode: Rectification of heat flux," **93**, 184301, number: 18 Reporter: Physical Review Letters.
[241]G. Wehmeyer, T. Yabuki, C. Monachon, J. Wu, and C. Dames, "Thermal diodes, regulators, and switches: Physical mechanisms and potential applications," **4**, 041304, number: 4 Reporter: Applied Physics Reviews.
[242]C. Dames, "Solid-state thermal rectification with existing bulk materials," **131**, 061301–061301–7, number: 6 Reporter: Journal of Heat Transfer.
[243]H. Wang, S. Hu, K. Takahashi, X. Zhang, H. Takamatsu, and J. Chen, "Experimental study of thermal rectification in suspended monolayer graphene," **8**, 15843 (), reporter: Nature Communications.

[244]D. L. Duong, S. J. Yun, and Y. H. Lee, "van der waals layered materials: Opportunities and challenges," **11**, 11803–11830, publisher: American Chemical Society.
[245]A. K. Geim and I. V. Grigorieva, "Van der waals heterostructures," **499**, 419–425, number: 7459 Publisher: Nature Publishing Group.
[246]X. Gu, Y. Wei, X. Yin, B. Li, and R. Yang, "Colloquium: Phononic thermal properties of two-dimensional materials," **90**, 041002, number: 4 Reporter: Reviews of Modern Physics.
[247]K. v. Klitzing, G. Dorda, and M. Pepper, "New method for high-accuracy determination of the fine-structure constant based on quantized hall resistance," Phys. Rev. Lett. **45**, 494–497 (1980).
[248]B. A. Bernevig, T. L. Hughes, and S.-C. Zhang, "Quantum spin hall effect and topological phase transition in hgte quantum wells," Science **314**, 1757–1761 (2006), https://science.sciencemag.org/content/314/5806/1757.full.pdf.
[249]W. Yao, D. Xiao, and Q. Niu, "Valley-dependent optoelectronics from inversion symmetry breaking," Phys. Rev. B **77**, 235406 (2008).
[250]L. Ju, Z. Shi, N. Nair, Y. Lv, C. Jin, J. Velasco, C. Ojeda-Aristizabal, H. A. Bechtel, M. C. Martin, A. Zettl, J. Analytis, and F. Wang, "Topological valley transport at bilayer graphene domain walls," Nature **520**, 650–655 (2015).
[251]J. E. Moore, "The birth of topological insulators," Nature **464**, 194–198 (2010).
[252]N. P. Armitage, E. J. Mele, and A. Vishwanath, "Weyl and dirac semimetals in three-dimensional solids," Rev. Mod. Phys. **90**, 015001 (2018).
[253]X. Wan, A. M. Turner, A. Vishwanath, and S. Y. Savrasov, "Topological semimetal and fermi-arc surface states in the electronic structure of pyrochlore iridates," Phys. Rev. B **83**, 205101 (2011).
[254]H. Weng, C. Fang, Z. Fang, B. A. Bernevig, and X. Dai, "Weyl semimetal phase in noncentrosymmetric transition-metal monophosphides," Phys. Rev. X **5**, 011029 (2015).
[255]S.-Y. Xu, C. Liu, S. K. Kushwaha, R. Sankar, J. W. Krizan, I. Belopolski, M. Neupane, G. Bian, N. Alidoust, T.-R. Chang, H.-T. Jeng, C.-Y. Huang, W.-F. Tsai, H. Lin, P. P. Shibayev, F.-C. Chou, R. J. Cava, and M. Z. Hasan, "Observation of fermi arc surface states in a topological metal," Science **347**, 294–298 (2015), https://science.sciencemag.org/content/347/6219/294.full.pdf.
[256]S.-Y. Xu, I. Belopolski, D. S. Sanchez, C. Zhang, G. Chang, C. Guo, G. Bian, Z. Yuan, H. Lu, T.-R. Chang, P. P. Shibayev, M. L. Prokopovych, N. Alidoust, H. Zheng, C.-C. Lee, S.-M. Huang, R. Sankar, F. Chou, C.-H. Hsu, H.-T. Jeng, A. Bansil, T. Neupert, V. N. Strocov, H. Lin, S. Jia, and M. Z. Hasan, "Experimental discovery of a topological weyl semimetal state in tap," Science Advances **1** (2015), 10.1126/sciadv.1501092, https://advances.sciencemag.org/content/1/10/e1501092.full.pdf.
[257]T. Kitagawa, E. Berg, M. Rudner, and E. Demler, "Topological characterization of periodically driven quantum systems," Phys. Rev. B **82**, 235114 (2010).
[258]N. H. Lindner, G. Refael, and V. Galitski, "Floquet topological insulator in semiconductor quantum wells," Nature Physics **7**, 490–495 (2011).
[259]Z. Fang, N. Nagaosa, K. S. Takahashi, A. Asamitsu, R. Mathieu, T. Ogasawara, H. Yamada, M. Kawasaki, Y. Tokura, and K. Terakura, "The anomalous hall effect and magnetic monopoles in momentum space," Science **302**, 92–95 (2003), https://science.sciencemag.org/content/302/5642/92.full.pdf.
[260]W. Xi and W. Ku, "Hunting down magnetic monopoles in two-dimensional topological insulators and superconductors," Phys. Rev. B **100**, 121201 (2019).
[261]A. Uri, Y. Kim, K. Bagani, C. K. Lewandowski, S. Grover, N. Auerbach, E. O. Lachman, Y. Myasoedov, T. Taniguchi, K. Watanabe, J. Smet, and E. Zeldov, "Nanoscale imaging of equilibrium quantum Hall edge currents and of the magnetic monopole response in graphene," Nature Physics **16**, 164–170 (2020).
[262]Z. Wang, Y. Chong, J. D. Joannopoulos, and M. Soljačić, "Observation of unidirectional backscattering-immune topological electromagnetic states," Nature **461**, 772–775 (2009).
[263]L. Lu, J. D. Joannopoulos, and M. Soljačić, "Topological photonics," Nature Photonics **8**, 821–829 (2014).
[264]T. Ozawa, H. M. Price, A. Amo, N. Goldman, M. Hafezi, L. Lu, M. C. Rechtsman, D. Schuster, J. Simon, O. Zilberberg, and I. Carusotto, "Topological photonics," Rev. Mod. Phys. **91**, 015006 (2019).
[265]R. Fleury, D. L. Sounas, C. F. Sieck, M. R. Haberman, and A. Alù, "Sound isolation and giant linear nonreciprocity in a compact acoustic circulator," Science **343**, 516–519 (2014), https://science.sciencemag.org/content/343/6170/516.full.pdf.
[266]X. Zhang, M. Xiao, Y. Cheng, M.-H. Lu, and J. Christensen, "Topological sound," Communications Physics **1**, 97 (2018).
[267]Y. Wu, M. Yang, and P. Sheng, "Perspective: Acoustic metamaterials in transition," Journal of Applied Physics **123**, 090901 (2018), https://doi.org/10.1063/1.5007682.
[268]Y. Liu, X. Chen, and Y. Xu, "Topological phononics: From fundamental models to real materials," Advanced Functional Materials **30**, 1904784 (2020), https://onlinelibrary.wiley.com/doi/pdf/10.1002/adfm.201904784.
[269]R. Resta, "Manifestations of berry's phase in molecules and condensed matter," Journal of Physics: Condensed Matter **12**, R107–R143 (2000).
[270]D. Xiao, M.-C. Chang, and Q. Niu, "Berry phase effects on electronic properties," Rev. Mod. Phys. **82**, 1959–2007 (2010).
[271]M. Fruchart and D. Carpentier, "An introduction to topological insulators," Comptes Rendus Physique **14**, 779 – 815 (2013), topological insulators / Isolants topologiques.
[272]D. J. Thouless, M. Kohmoto, M. P. Nightingale, and M. den Nijs, "Quantized hall conductance in a two-dimensional periodic potential," Phys. Rev. Lett. **49**, 405–408 (1982).
[273]Z. Zhang, Y. Tian, Y. Cheng, Q. Wei, X. Liu, and J. Christensen, "Topological acoustic delay line," Phys. Rev. Applied **9**, 034032 (2018).
[274]H. Gao, H. Xue, Q. Wang, Z. Gu, T. Liu, J. Zhu, and B. Zhang, "Observation of topological edge states induced solely by non-hermiticity in an acoustic crystal," Phys. Rev. B **101**, 180303 (2020).
[275]I. Kim, S. Iwamoto, and Y. Arakawa, "Topologically protected elastic waves in one-dimensional phononic crystals of continuous media," Applied Physics Express **11**, 017201 (2017).
[276]X. Fan, C. Qiu, Y. Shen, H. He, M. Xiao, M. Ke, and Z. Liu, "Probing weyl physics with one-dimensional sonic crystals," Phys. Rev. Lett. **122**, 136802 (2019).
[277]Z. Zhang, H. Long, C. Liu, C. Shao, Y. Cheng, X. Liu, and J. Christensen, "Deep-subwavelength holey acoustic second-order topological insulators," Advanced Materials **31**, 1904682 (2019), https://onlinelibrary.wiley.com/doi/pdf/10.1002/adma.201904682.
[278]J.-P. Xia, D. Jia, H.-X. Sun, S.-Q. Yuan, Y. Ge, Q.-R. Si, and X.-J. Liu, "Programmable coding acoustic topological insulator," Advanced Materials **30**, 1805002 (2018), https://onlinelibrary.wiley.com/doi/pdf/10.1002/adma.201805002.
[279]Z. Tian, C. Shen, J. Li, E. Reit, H. Bachman, J. E. S. Socolar, S. A. Cummer, and T. Jun Huang, "Dispersion tuning and route reconfiguration of acoustic waves in valley topological phononic crystals," Nature Communications **11**, 762 (2020).
[280]Z. Zhang, Y. Tian, Y. Wang, S. Gao, Y. Cheng, X. Liu, and J. Christensen, "Directional acoustic antennas based on valley-hall topological insulators," Advanced Materials **30**, 1803229 (2018), https://onlinelibrary.wiley.com/doi/pdf/10.1002/adma.201803229.
[281]Y.-G. Peng, C.-Z. Qin, D.-G. Zhao, Y.-X. Shen, X.-Y. Xu, M. Bao, H. Jia, and X.-F. Zhu, "Experimental demonstration of anomalous Floquet topological insulator for sound," Nature Communications **7**, 13368 (2016).
[282]D. Jia, H. xiang Sun, J. ping Xia, S. qi Yuan, X. jun Liu, and C. Zhang, "Acoustic topological insulator by honeycomb sonic crystals with direct and indirect band gaps," New Journal of Physics **20**, 093027 (2018).
[283]D. Jia, H. xiang Sun, S. qi Yuan, C. Zhang, and X. jun Liu, "Pseudospin-dependent acoustic topological insulator by airborne sonic crystals with a triangular lattice," Applied Physics Express **12**, 044003 (2019).
[284]Q. Wei, Y. Tian, S.-Y. Zuo, Y. Cheng, and X.-J. Liu, "Experimental demonstration of topologically protected efficient sound propagation in an acoustic waveguide network," Phys. Rev. B **95**, 094305 (2017).
[285]B.-Z. Xia, T.-T. Liu, G.-L. Huang, H.-Q. Dai, J.-R. Jiao, X.-G. Zang, D.-J. Yu, S.-J. Zheng, and J. Liu, "Topological phononic insulator with robust pseudospin-dependent transport," Phys. Rev. B **96**, 094106 (2017).
[286]C. He, X. Ni, H. Ge, X.-C. Sun, Y.-B. Chen, M.-H. Lu, X.-P. Liu, and Y.-F. Chen, "Acoustic topological insulator and robust one-way sound transport," Nature Physics **12**, 1124–1129 (2016).
[287]Z. Zhang, Y. Tian, Y. Cheng, X. Liu, and J. Christensen, "Experimental verification of acoustic pseudospin multipoles in a symmetry-broken snowflakelike topological insulator," Phys. Rev. B **96**, 241306 (2017).

[288] Y. Deng, H. Ge, Y. Tian, M. Lu, and Y. Jing, "Observation of zone folding induced acoustic topological insulators and the role of spin-mixing defects," Phys. Rev. B **96**, 184305 (2017).
[289] H. Dai, M. Qian, J. Jiao, B. Xia, and D. Yu, "Subwavelength acoustic topological edge states realized by zone folding and the role of boundaries selection," Journal of Applied Physics **124**, 175107 (2018), https://doi.org/10.1063/1.5051377.
[290] Q. Zhang, Y. Chen, K. Zhang, and G. Hu, "Dirac degeneracy and elastic topological valley modes induced by local resonant states," Phys. Rev. B **101**, 014101 (2020).
[291] S.-y. Huo, J.-j. Chen, H.-b. Huang, and G.-l. Huang, "Simultaneous multi-band valley-protected topological edge states of shear vertical wave in two-dimensional phononic crystals with veins," Scientific Reports **7**, 10335 (2017).
[292] H. Xue, Y. Yang, F. Gao, Y. Chong, and B. Zhang, "Acoustic higher-order topological insulator on a kagome lattice," Nature Materials **18**, 108–112 (2019).
[293] B. Xie, H. Liu, H. Cheng, Z. Liu, S. Chen, and J. Tian, "Acoustic topological transport and refraction in a kekulé lattice," Phys. Rev. Applied **11**, 044086 (2019).
[294] B.-Z. Xia, S.-J. Zheng, T.-T. Liu, J.-R. Jiao, N. Chen, H.-Q. Dai, D.-J. Yu, and J. Liu, "Observation of valleylike edge states of sound at a momentum away from the high-symmetry points," Phys. Rev. B **97**, 155124 (2018).
[295] Z. Zhu, X. Huang, J. Lu, M. Yan, F. Li, W. Deng, and Z. Liu, "Negative refraction and partition in acoustic valley materials of a square lattice," Phys. Rev. Applied **12**, 024007 (2019).
[296] Z. Yang, F. Gao, and B. Zhang, "Topological water wave states in a one-dimensional structure," Scientific Reports **6**, 29202 (2016).
[297] P. Delplace, J. B. Marston, and A. Venaille, "Topological origin of equatorial waves," Science **358**, 1075–1077 (2017), https://science.sciencemag.org/content/358/6366/1075.full.pdf.
[298] N. Laforge, V. Laude, F. Chollet, A. Khelif, M. Kadic, Y. Guo, and R. Fleury, "Observation of topological gravity-capillary waves in a water wave crystal," New Journal of Physics **21**, 083031 (2019).
[299] M. P. Makwana, N. Laforge, R. V. Craster, G. Dupont, S. Guenneau, V. Laude, and M. Kadic, "Experimental observations of topologically guided water waves within non-hexagonal structures," Applied Physics Letters **116**, 131603 (2020), https://doi.org/10.1063/1.5141850.
[300] C. He, S.-Y. Yu, H. Ge, H. Wang, Y. Tian, H. Zhang, X.-C. Sun, Y. B. Chen, J. Zhou, M.-H. Lu, and Y.-F. Chen, "Three-dimensional topological acoustic crystals with pseudospin-valley coupled saddle surface states," Nature Communications **9**, 4555 (2018).
[301] C. He, H.-S. Lai, B. He, S.-Y. Yu, X. Xu, M.-H. Lu, and Y.-F. Chen, "Acoustic analogues of three-dimensional topological insulators," Nature Communications **11**, 2318 (2020).
[302] H. He, C. Qiu, L. Ye, X. Cai, X. Fan, M. Ke, F. Zhang, and Z. Liu, "Topological negative refraction of surface acoustic waves in a Weyl phononic crystal," Nature **560**, 61–64 (2018).
[303] Y. Qi, C. Qiu, M. Xiao, H. He, M. Ke, and Z. Liu, "Acoustic realization of quadrupole topological insulators," Phys. Rev. Lett. **124**, 206601 (2020).
[304] X. Ni, M. Li, M. Weiner, A. Alù, and A. B. Khanikaev, "Demonstration of a quantized acoustic octupole topological insulator," Nature Communications **11**, 2108 (2020).
[305] H. Xue, Y. Ge, H.-X. Sun, Q. Wang, D. Jia, Y.-J. Guan, S.-Q. Yuan, Y. Chong, and B. Zhang, "Observation of an acoustic octupole topological insulator," Nature Communications **11**, 2442 (2020).
[306] A. Merkel and J. Christensen, "Ultrasonic nodal chains in topological granular metamaterials," Communications Physics **2**, 154 (2019).
[307] Y.-G. Peng, Y. Li, Y.-X. Shen, Z.-G. Geng, J. Zhu, C.-W. Qiu, and X.-F. Zhu, "Chirality-assisted three-dimensional acoustic floquet lattices," Phys. Rev. Research **1**, 033149 (2019).
[308] Y. Fu, C. Shen, X. Zhu, J. Li, Y. Liu, S. A. Cummer, and Y. Xu, "Sound vortex diffraction via topological charge in phase gradient metagratings," Science Advances **6** (2020), 10.1126/sciadv.aba9876, https://advances.sciencemag.org/content/6/40/eaba9876.full.pdf.
[309] X. Zhu, K. Li, P. Zhang, J. Zhu, J. Zhang, C. Tian, and S. Liu, "Implementation of dispersion-free slow acoustic wave propagation and phase engineering with helical-structured metamaterials," Nature Communications **7**, 11731 (2016).
[310] H. Xue, Y. Yang, G. Liu, F. Gao, Y. Chong, and B. Zhang, "Realization of an acoustic third-order topological insulator," Phys. Rev. Lett. **122**, 244301 (2019).
[311] A. Song, J. Li, C. Shen, T. Chen, and S. A. Cummer, "Switchable directional sound emission with improved field confinement based on topological insulators," Applied Physics Letters **117**, 043503 (2020), https://doi.org/10.1063/5.0012290.
[312] M. Makwana, R. Craster, and S. Guenneau, "Topological beam-splitting in photonic crystals," Opt. Express **27**, 16088–16102 (2019).
[313] Y. Tang, Y. Zhu, B. Liang, J. Yang, J. Yang, and J. Cheng, "One-way Acoustic Beam Splitter," Scientific Reports **8**, 13573 (2018).
[314] T. Liu, G. Ma, S. Liang, H. Gao, Z. Gu, S. An, and J. Zhu, "Single-sided acoustic beam splitting based on parity-time symmetry," Phys. Rev. B **102**, 014306 (2020).
[315] M. P. Makwana and G. Chaplain, "Tunable three-way topological energy-splitter," Scientific Reports **9**, 18939 (2019).
[316] P. Wang, L. Lu, and K. Bertoldi, "Topological phononic crystals with one-way elastic edge waves," Phys. Rev. Lett. **115**, 104302 (2015).
[317] J. Lu, C. Qiu, L. Ye, X. Fan, M. Ke, F. Zhang, and Z. Liu, "Observation of topological valley transport of sound in sonic crystals," Nature Physics **13**, 369–374 (2017).
[318] Y. Ding, Y. Peng, Y. Zhu, X. Fan, J. Yang, B. Liang, X. Zhu, X. Wan, and J. Cheng, "Experimental demonstration of acoustic chern insulators," Phys. Rev. Lett. **122**, 014302 (2019).
[319] Y. Huang, X. Wang, X. Gong, H. Wu, D. Zhang, and D. Zhang, "Contact Nonlinear Acoustic Diode," Scientific Reports **10**, 2564 (2020).
[320] J. Zhu, X. Zhu, X. Yin, Y. Wang, and X. Zhang, "Unidirectional extraordinary sound transmission with mode-selective resonant materials," Phys. Rev. Applied **13**, 041001 (2020).
[321] M. Wang, W. Zhou, L. Bi, C. Qiu, M. Ke, and Z. Liu, "Valley-locked waveguide transport in acoustic heterostructures," Nature Communications **11**, 3000 (2020).
[322] R. Ganesh and S. Gonella, "From modal mixing to tunable functional switches in nonlinear phononic crystals," Phys. Rev. Lett. **114**, 054302 (2015).
[323] M. S. Rudner and N. H. Lindner, "Band structure engineering and non-equilibrium dynamics in Floquet topological insulators," Nature Reviews Physics **2**, 229–244 (2020).
[324] S. Li, D. Zhao, H. Niu, X. Zhu, and J. Zang, "Observation of elastic topological states in soft materials," Nature Communications **9**, 1370 (2018).
[325] M. Esmann, F. R. Lamberti, A. Lemaître, and N. D. Lanzillotti-Kimura, "Topological acoustics in coupled nanocavity arrays," Phys. Rev. B **98**, 161109 (2018).
[326] M. Esmann, F. R. Lamberti, P. Senellart, I. Favero, O. Krebs, L. Lanco, C. Gomez Carbonell, A. Lemaître, and N. D. Lanzillotti-Kimura, "Topological nanophononic states by band inversion," Phys. Rev. B **97**, 155422 (2018).
[327] G. Arregui, O. Ortíz, M. Esmann, C. M. Sotomayor-Torres, C. Gomez-Carbonell, O. Mauguin, B. Perrin, A. Lemaître, P. D. García, and N. D. Lanzillotti-Kimura, "Coherent generation and detection of acoustic phonons in topological nanocavities," APL Photonics **4**, 030805 (2019), https://doi.org/10.1063/1.5082728.
[328] S. Yves, R. Fleury, F. Lemoult, M. Fink, and G. Lerosey, "Topological acoustic polaritons: robust sound manipulation at the subwavelength scale," New Journal of Physics **19**, 075003 (2017).
[329] S. Anguiano, A. E. Bruchhausen, B. Jusserand, I. Favero, F. R. Lamberti, L. Lanco, I. Sagnes, A. Lemaître, N. D. Lanzillotti-Kimura, P. Senellart, and A. Fainstein, "Micropillar resonators for optomechanics in the extremely high 19–95-ghz frequency range," Phys. Rev. Lett. **118**, 263901 (2017).
[330] F. R. Lamberti, Q. Yao, L. Lanco, D. T. Nguyen, M. Esmann, A. Fainstein, P. Sesin, S. Anguiano, V. V. ne, A. Bruchhausen, P. Senellart, I. Favero, and N. D. Lanzillotti-Kimura, "Optomechanical properties of gaas/alas micropillar resonators operating in the 18 ghz range," Opt. Express **25**, 24437–24447 (2017).
[331] W. Wang, Y. Jin, W. Wang, B. Bonello, B. Djafari-Rouhani, and R. Fleury, "Robust fano resonance in a topological mechanical beam," Phys. Rev. B **101**, 024101 (2020).
[332] W. Wang, B. Bonello, B. Djafari-Rouhani, and Y. Pennec, "Topological valley, pseudospin, and pseudospin-valley protected edge states in symmetric pillared phononic crystals," Phys. Rev. B **100**, 140101 (2019).

[333] W. Wang, B. Bonello, B. Djafari-Rouhani, and Y. Pennec, "Polarization-dependent and valley-protected lamb waves in asymmetric pillared phononic crystals," Journal of Physics D: Applied Physics **52**, 505302 (2019).

[334] P. Ruello and V. E. Gusev, "Physical mechanisms of coherent acoustic phonons generation by ultrafast laser action," Ultrasonics **56**, 21 – 35 (2015).

[335] B. Graczykowski, A. Gueddida, B. Djafari-Rouhani, H.-J. Butt, and G. Fytas, "Brillouin light scattering under one-dimensional confinement: Symmetry and interference self-canceling," Phys. Rev. B **99**, 165431 (2019).

[336] B. Graczykowski, M. Sledzinska, M. Placidi, D. Saleta Reig, M. Kasprzak, F. Alzina, and C. M. Sotomayor Torres, "Elastic Properties of Few Nanometers Thick Polycrystalline MoS2 Membranes: A Nondestructive Study," Nano Letters **17**, 7647–7651 (2017), publisher: American Chemical Society.

[337] T. Marchesi D'Alvise, S. Harvey, L. Hueske, J. Szelwicka, L. Veith, T. P. J. Knowles, D. Kubiczek, C. Flaig, F. Port, K.-E. Gottschalk, F. Rosenau, B. Graczykowski, G. Fytas, F. S. Ruggeri, K. Wunderlich, and T. Weil, "Ultrathin polydopamine films with phospholipid nanodiscs containing a glycophorin a domain," Advanced Functional Materials **30**, 2000378 (2020), https://onlinelibrary.wiley.com/doi/pdf/10.1002/adfm.202000378.

[338] Y. Xu, X. Tian, and C. Chen, "Band structures of two dimensional solid/air hierarchical phononic crystals," Physica B: Condensed Matter **407**, 1995 – 2001 (2012).

[339] K. Hur, R. G. Hennig, and U. Wiesner, "Exploring Periodic Bicontinuous Cubic Network Structures with Complete Phononic Bandgaps," The Journal of Physical Chemistry C **121**, 22347–22352 (2017), publisher: American Chemical Society.

[340] C.-Y. Lee, M. J. Leamy, and J. H. Nadler, "Frequency band structure and absorption predictions for multi-periodic acoustic composites," Journal of Sound and Vibration **329**, 1809 – 1822 (2010).

[341] M. I. HUSSEIN, K. Hamza, G. M. Hulbert, and K. Saitou, "Optimal synthesis of 2d phononic crystals for broadband frequency isolation," Waves in Random and Complex Media **17**, 491–510 (2007), https://doi.org/10.1080/17455030701501869.

[342] Y. f. Li, X. Huang, F. Meng, and S. Zhou, "Evolutionary topological design for phononic band gap crystals," Structural and Multidisciplinary Optimization **54**, 595–617 (2016).

[343] Z.-x. Xu, H. Gao, Y.-j. Ding, J. Yang, B. Liang, and J.-c. Cheng, "Topology-optimized omnidirectional broadband acoustic ventilation barrier," Phys. Rev. Applied **14**, 054016 (2020).

[344] S. M. Sadat and R. Y. Wang, "A machine learning based approach for phononic crystal property discovery," Journal of Applied Physics **128**, 025106 (2020), https://doi.org/10.1063/5.0006153.

[345] C. Choi, S. Bansal, N. Münzenrieder, and S. Subramanian, "Fabricating and assembling acoustic metamaterials and phononic crystals," Advanced Engineering Materials **n/a**, 2000988, https://onlinelibrary.wiley.com/doi/pdf/10.1002/adem.202000988.

[346] X. Wang, X. Luo, B. Yang, and Z. Huang, "Ultrathin and durable open metamaterials for simultaneous ventilation and sound reduction," Applied Physics Letters **115**, 171902 (2019), https://doi.org/10.1063/1.5121366.

[347] T. Delpero, S. Schoenwald, A. Zemp, and A. Bergamini, "Structural engineering of three-dimensional phononic crystals," Journal of Sound and Vibration **363**, 156 – 165 (2016).

[348] Y. Ge, H.-x. Sun, S.-q. Yuan, and Y. Lai, "Switchable omnidirectional acoustic insulation through open window structures with ultrathin metasurfaces," Phys. Rev. Materials **3**, 065203 (2019).

[349] Y. Ge, H.-x. Sun, S.-q. Yuan, and Y. Lai, "Broadband unidirectional and omnidirectional bidirectional acoustic insulation through an open window structure with a metasurface of ultrathin hooklike meta-atoms," Applied Physics Letters **112**, 243502 (2018), https://doi.org/10.1063/1.5025812.

[350] P. Wang, T.-N. Chen, K.-P. Yu, and X.-P. Wang, "Lamb wave band gaps in a double-sided phononic plate," Journal of Applied Physics **113**, 053509 (2013), https://doi.org/10.1063/1.4790301.

[351] A.-L. Song, T.-N. Chen, X.-P. Wang, and L.-L. Wan, "Waveform-preserved unidirectional acoustic transmission based on impedance-matched acoustic metasurface and phononic crystal," Journal of Applied Physics **120**, 085106 (2016), https://doi.org/10.1063/1.4961659.

[352] Y. Xiao, J. Wen, L. Huang, and X. Wen, "Analysis and experimental realization of locally resonant phononic plates carrying a periodic array of beam-like resonators," Journal of Physics D: Applied Physics **47**, 045307 (2013).

[353] L. Li, X. Gang, Z. Sun, X. Zhang, and F. Zhang, "Design of phononic crystals plate and application in vehicle sound insulation," Advances in Engineering Software **125**, 19 – 26 (2018).

[354] H. Ryoo and W. Jeon, "Dual-frequency sound-absorbing metasurface based on visco-thermal effects with frequency dependence," Journal of Applied Physics **123**, 115110 (2018), https://doi.org/10.1063/1.5017540.

[355] M. Duan, C. Yu, Z. Xu, F. Xin, and T. J. Lu, "Acoustic impedance regulation of helmholtz resonators for perfect sound absorption via roughened embedded necks," Applied Physics Letters **117**, 151904 (2020), https://doi.org/10.1063/5.0024804.

[356] R. Ghaffarivardavagh, J. Nikolajczyk, S. Anderson, and X. Zhang, "Ultra-open acoustic metamaterial silencer based on fano-like interference," Phys. Rev. B **99**, 024302 (2019).

[357] R. Martínez-Sala, C. Rubio, L. M. García-Raffi, J. V. Sánchez-Pérez, E. A. Sánchez-Pérez, and J. Llinares, "Control of noise by trees arranged like sonic crystals," Journal of Sound and Vibration **291**, 100 – 106 (2006).

[358] S. Zou, Y. Xu, R. Zatianina, C. Li, X. Liang, L. Zhu, Y. Zhang, G. Liu, Q. H. Liu, H. Chen, and Z. Wang, "Broadband waveguide cloak for water waves," Phys. Rev. Lett. **123**, 074501 (2019).

[359] C. Li, L. Xu, L. Zhu, S. Zou, Q. H. Liu, Z. Wang, and H. Chen, "Concentrators for water waves," Phys. Rev. Lett. **121**, 104501 (2018).